EXPERIMENTAL STUDIES OF BEACH SCOUR DUE TO WAVE ACTION

by

Won Oh Song and Robert E. Schiller
Coastal, Hydraulic, and Ocean Engineering Group
Civil Engineering Department
Texas A&M University

July 1973

TAMU-SG-73-211

Partially Supported by the
National Oceanic and Atmospheric
Administration Sea Grant Program
Department of Commerce Grants:
2-35213 1971-72
04-3-158-18 1972-73

Coastal, Hydraulic, and Ocean Engineering Group
Report No. 166 C.O.E.

ABSTRACT

A series of experiments was conducted to investigate the processes involved in the formation of beach scour, caused by wave action, on a natural beach and a seawall beach. The studies also took into account the determination of the reflection coefficient which characterized the wave reflected from both the seawall and the deformed beach profile. The standing wave, formed by the reflection of the waves, was found to be important in the analysis of beach scour phenomena.

For the calculation of the reflection coefficient, two methods were used: the envelope method and the Coastal Engineering Research Center (CERC) method. The results given by the two methods showed excellent agreement.

The linear standing wave theory was compared with the second order standing wave theory. The wave surface profile and the corresponding horizontal and vertical velocity components of the water particles at the designated points on the free water surface were calculated on the basis of the two theories. The results of the comparisons indicate that the linear standing wave theory gives good results as a first approximation; therefore, it was used in this study. To predict the scour depth on the natural beach and the seawall beach, regression analyses were performed. The results gave excellent correlation.

PREFACE

In 1969 an experimental study of beach scour was initiated by Charles Chesnutt and Robert E. Schiller. Beach scour as a function of beach slope, sea wall inclination and location was studied in two wave channels. This study was reported on in C.O.E. Report No. 139 of May 1971.

The present experimental work was begun in May 1971 and is an extension of the earlier experimental work on beach scour.

The report was primarily written by the senior author in partial fulfillment of the Doctor of Philosophy requirement under the supervision of the junior author who was his major advisor.

The reviews of this report by Dr. T.J. Kozik, Dr. L.L. Lowery, Jr., Dr. J.E. Martinez, and Dr. John B. Herbich; assistance by Mr. Charles Chessnut, Mr. George Owens, and Mr. Paul Versowsky during the experimental program; and computer programs supplied by Mr. J.C. Ahlquist are gratefully acknowledged.

This two year study was partially funded by National Oceanic and Atmospheric Administration Sea Grant Program, Department of Commerce grants 2-35213 and 04-3-158-18.

TABLE OF CONTENTS

TABLE OF CONTENTS (cont.)

LIST OF FIGURES

LIST OF FIGURES (CONTINUED)

LIST OF TABLES

INTRODUCTION

The purpose of these experimental studies is to investigate scour phenomena, caused by wave action, on a natural beach and a seawall beach. The relationships between scour depth at the toe of a beach protected by a seawall and the characteristics of the approaching waves, the beach faces, and the seawall itself are more difficult to define precisely. No theoretical method for predicting the scour depth has so far been developed. Hence, this study is primarily directed toward an experimental rather than a theoretical approach. The present rule of thumb method for this is that "the maximum depth of scour trough below the natural bed may be approximated as being equal to the height of the maximum unbroken wave that can be supported by the original depth of water at the toe of the structure" (38).

In practice, the erosion at the toe of coastal structures, such as seawalls, breakwaters, revetments, etc., has caused them to be damaged or to collapse. The accretion in front of these structures has required unnecessary dredging for navigation. Both erosion and accretion present problems to coastal engineers.

A movable model beach was constructed in a two dimensional wave tank where the beach was subjected to a series of monochromatic

---

The citations on the following pages follow the style of the Journal of the Waterways, Harbors and Coastal Engineering Division of the American Society of Civil Engineers.

progressive waves. As the wave action progressed, the beach profile was changed, and so were the characteristics of the waves.

For the natural beach tests, wave action was continued for 48 hours, resulting in a relatively stable beach profile; a seawall was then erected at selected points on the beach. As a result, the scour depth at the toe of the seawall and the pattern of the beach profile changed. These changes are caused by the reflection of the waves from the seawall and the beach.

The next step was to calculate the reflection coefficient of a standing wave. The Coastal Engineering Research Center (CERC) method was employed, and the results were compared with the envelope method. Excellent agreement took place.

The linear standing wave theory was compared with the second order standing wave theory. The wave surface profile, and the corresponding horizontal and vertical velocity components of the water particles at the designated points on the free water surface were calculated on the basis of the two wave theories. The results of the comparison indicate that the linear standing wave theory gives good results as a first approximation; therefore, it was used in this study.

To predict the scour depth on the natural beach and the seawall beach, regression analyses were performed. The results gave excellent correlation.

LITERATURE SURVEY

Fixed Bed Studies

A number of studies have been made to investigate the reflecting capacity of different kinds of slopes on waves.

Iribarren and Nogales (15) made experimental studies on the slope producing a complete breaking or total reflection of the oncoming waves from the slopes. They defined the critical slope angle giving the reflection coefficient of 50% as

$$(\tan \alpha)_{crit} = \frac{8}{T} \sqrt{H/2g}$$

where α = slope angle,

T = wave period,

H = wave height, and

g = acceleration of gravity.

Miche (24) made theoretical studies on the wave steepness producing a complete reflection of the oncoming waves from a gently sloping plane. He defined the critical wave steepness associated with the total reflection as

$$(Ho/Lo)_{crit} = \sqrt{2\alpha/\pi} \quad \frac{\sin^2 \alpha}{\pi}$$

where Ho = deep water wave height,

Lo = deep water wave length, and

$\pi = 3.14159...$

For higher wave steepness, the incident wave will be broken in front of the plane and partially reflected. He defined the theoretical reflection coefficient as

$$R' = 1 \qquad \text{for } Ho/Lo \leq (Ho/Lo)_{crit}$$

$$R' = \frac{(Ho/Lo)_{crit}}{Ho/Lo} \qquad \text{for } Ho/Lo \geq (Ho/Lo)_{crit}$$

where R' = theoretical reflection coefficient.

The theoretical reflection coefficient was modified by using the intrinsic reflection coefficient given by the surface roughness of the slopes. The reflection coefficient was defined as

$$R = \rho R'$$

where R = reflection coefficient, and

ρ = intrinsic reflection coefficient.

The theory was verified experimentally by Healy (10); Ursell, Dean, and Yu (37); and Schoemaker and Thijsse (35).

Those studies were confined to the reflection from an inclined or vertical wall on a fixed bed. Thus, they did not consider the effect of the change of the bottom profile on the wave reflection. Reflection studies with movable beds more nearly simulate natural conditions than do the fixed bed studies; however, the variation of the reflection due to the beach profile change introduces more variables into the reflection studies, and further complicates the problem.

Movable Bed Studies

Russell and Inglis (31) studied the influence of a vertical wall on a stable beach under the action of waves and tides. They observed that the reflected wave made faster orbital movements of the water particles and thus increased erosion. The ultimate scour depth was found to be about one wave height below mean low water.

Hunt (14) viewed the wave reflection from a seawall as the most important factor to be considered in seawall design. He further suggested that to minimize the wave reflection, the slope of the seawall should be less than H/T^2.

Herbich, Murphy, and Van Weele (11) investigated the scour of a flat sand beach under nonbreaking wave conditions, using three different wall inclination angles. They found that the ultimate scour depth decreased generally with the decreasing angle of seawall inclination and reflection coefficient. Herbich and Ko (12) developed a mathematical model to determine the ultimate scour depth on a flat beach. The results were compared with subsequent laboratory measurements, and a reasonably good agreement was obtained.

Sawagari (34) investigated the scour depth at the toe of a permeable wall. He found that the reflection coefficient was related directly to the permeability of the seawall and the scour depth.

Sato, Tanaka and Irie (33) conducted intensive laboratory and field investigations to clarify the basic beach scour characteristics around coastal structures. Four types of scour patterns were classified, depending upon the manner in which the scouring process

progressed. Currents induced by wave breaking were observed as a significant variable in the scour around the structure.

Herbich (13) summarized the state-of-the-art of beach scour studies, and tried to correlate the relationships between wave characteristics and beach scour patterns with field data from the Texas Gulf Coast.

Chesnutt and Schiller (3) investigated the effect of relative seawall distance (the ratio of the position of seawall with respect to the position of breaking wave) and the inclination angles of the seawall on the scour depth of sloping beaches. They concluded that the effect of the relative seawall distance is as important to scour depth as is wave height.

In the previous beach scour studies, the relationship between scour depth and related variables was qualitatively treated. The main purpose of this study is to correlate quantitatively those variables by using systematic experimental design and regression analysis.

REFLECTION COEFFICIENT

Measurement of Reflection

A standing wave system consists of two components, an incident wave and a reflected wave. The experimental method for the determination of the two components uses the record of the fluctuations of the wave profile as a function of time. The record is made by a wave probe, resistance or capacitance type, immersed partially in water and held at rest in a fixed vertical position.

To separate the two components of the standing wave, Keulegan (17) described two methods: one variable probe position method and fixed probe position method. It is assumed that the approaching waves are of sinusoidal wave form with a constant amplitude.

In the variable probe position method, one probe is moved along the wave tank between node and loop envelope points in several small steps. At each step, the probe is held at a given position for at least one wave period. The fluctuations of the wave profile are recorded (Fig. 1)*. The reflection coefficient is then defined as

$$\left(\frac{Ar}{Ai}\right)^2 = \left(\frac{\eta_\ell - \eta_n}{\eta_\ell + \eta_n}\right)^2$$

where Ai = amplitude of incident wave,

Ar = amplitude of reflected wave,

η_ℓ = amplitude of the surface profile at loop point, and

η_n = amplitude of the surface profile at node point.

*All figures are collected in Appendix C at the end of the paper.

In the fixed probe position method, two or three probes are placed along the channel axis. In the case of the two fixed probe method, probes 1 and 2 are located at two points, one-quarter wave length apart. Two simultaneous wave profiles (Fig. 2) at each probe are recorded. The reflection coefficient is defined as

$$\left(\frac{Ar}{Ai}\right)^2 = \frac{(\eta_{12} + \eta_{21})^2 + \eta_{22}^2}{(\eta_{12} - \eta_{21})^2 + \eta_{22}^2}$$

where η_{12} = deflection obtained from curve 1, corresponding to probe 1, for the instant t = T/4, and

η_{21}, η_{22} = deflections obtained from curve 2, corresponding to probe 2, for the instant t = 0 and T/4, respectively.

The origin of time is selected as one point of zero deflection of the record curve from probe 1.

If the probes are located at the loop and node points, the phase shift at the two points will be a one quarter wave period. As a result, η_{22} will vanish, and η_{12} and η_{21} will correspond to the η_ℓ and η_n of the variable probe position method, respectively. Consequently, the above two methods are equivalent from the point of view of the location of the probes.

In the case of the three fixed wave probe method, the third probe is located at the mid-point between the probe 1 and 2. Hence, three simultaneous wave profiles (Fig. 3) at each probe are recorded. This method is intended to eliminate the error caused by the determination of wave length in the two fixed probe method.

The reflection coefficient is defined as

$$\left(\frac{Ar}{Ai}\right)^2 = \frac{(\eta_{11} - \eta_{32})^2 + \eta_{31}^2}{(\eta_{11} + \eta_{32})^2 + \eta_{31}^2}$$

where η_{11} = deflection obtained from curve 1, corresponding to probe 1, for the instant t = 0, and

η_{31}, η_{32} = deflections obtained from curve 3, corresponding to probe 3, for the instant t = 0 and T/4, respectively.

The origin of time is selected as one point of maximum deflection of the record curve from probe 1.

Of these methods, Keulegan suggested that the three fixed probe method was superior to the others. However, laboratory experience gained during this study demonstrated Keulegan's three fixed wave probe method to be cumbersome to calibrate as well as creating problems in maintaining the several recording channels and wave probes for each run. Moreover, some errors caused by the inherent gage factor for each channel caused inconsistencies to occur in the data. Hence, the single moving probe method with multiple reading points on the envelope was used for this study.

Keulegan defined the reflection coefficient as $(Ar/Ai)^2$ which may also be defined as the energy ratio. For convenience of this study, however, the ratio of the amplitude of reflected wave to incident wave, Ar/Ai, was employed as a reflection coefficient. On the basis of the linear wave theory, the total energy in a wave per unit width of crest is

$$E = \frac{\gamma H^2 L}{8}$$

where E = total wave energy, and

γ = unit weight of water.

Consequently, the ratio of the energy of reflected wave to incident wave, Er/Ei, can be converted to the wave height ratio, Hr/Hi, as well as the amplitude ratio, Ar/Ai:

$$\frac{Er}{Ei} = \left(\frac{Hr}{Hi}\right)^2 = \left(\frac{Ar}{Ai}\right)^2$$

Calculation of Reflection Coefficient: Envelope Method

Any structures in the wave path cause reflection. If the reflected wave returns along the incident path, a standing wave results. The two components of this standing wave are the incident wave, η_i = Ai cos (mx-kt), and the reflected wave, η_r = Ar cos (mx+kt). The superposition of these two components results in a wave form of

$$\eta = (Ai+Ar) \cos (mx+kt) - 2Ar \sin mx \sin kt$$

The first term is of the monochromatic progressive wave form, and the second term is of the standing wave form.

Beat effects of these waves on the wave profile make envelopes with loop and node points, the distance between these two points being one-quarter wave length, L/4. The loop on the wave envelope is formed when a reflected wave crest meets an incident wave crest; the wave height of the loop envelope, Hl = 2(Ai+Ar), occurs at

$x = 0, L/2, L$, etc. The node is formed when a reflected wave crest meets an incident wave trough; the wave height of the node, $Hn = 2(Ai-Ar)$, occurs at $x = L/4, 3L/4$, etc. If $Ai = Ar$, the progressive wave term vanishes, and a perfect or pure standing wave is formed. If $Ar = 0$, the standing wave term vanishes, and a progressive wave is formed. For the intermediate case, $Ai > Ar$, the standing wave and progressive waves make a partial standing wave. Thus, use of the envelope method in the calculation of the reflection coefficient results in its definition as the amplitude ratio of the reflected wave to the incident wave:

$$R = \frac{Ar}{Ai}$$

$$Hi = 2Ai$$

$$Hr = 2Ar$$

$$H\ell = 2(Ai+Ar)$$

$$Hn = 2(Ai-Ar)$$

$$R = \frac{Hr}{Hi} = \frac{H\ell - Hn}{H\ell + Hn}$$

where Hi = incident wave height,

Hr = reflected wave height,

$H\ell$ = loop wave envelope height, and

Hn = node wave envelope height.

This method, called the envelope method or loop and node method, has been used for the calculation of the reflection coefficient. However, the wave generated in the wave tank was not always of the form of

ideal sinusoidal wave. The slightly irregular shape of the wave envelope raised problems in the determination of the wave height and reflection coefficient.

Calculation of Reflection Coefficient: CERC Method

A new method of calculation of the reflection coefficient was developed by the Coastal Engineering Research Center (CERC). This method considers the whole wave envelope height in order to eliminate the error involved in using only the node and loop envelope heights. Unlike the envelope method, the actually collected envelope was processed statistically to obtain the mean wave height and the best fit sine curve for the envelope. To calculate the reflection coefficient, two computer programs, WHVTCN and WHVTC2, were set up. (WHV stands for wave height variability.) The original computer programs written by Ahlquist and James (1) of CERC were modified for this investigation.

Fig. 4 shows a full length of a wave envelope record collected in the wave channel. The x- and y- coordinates were digitized to two decimal points of one inch, and were keypunched for input data for the program WHVTCN.

The following are the general outlines for the above two programs:

The program WHVTCN edits the digitized data points, and converts them to actual wave height. The y- coordinate scale ratio of 3.0 in./in. was used to calculate the wave height; however, the x-coordinate scale ratio varied with the travel speed of the wave probe.

The x-values were multiplied by linear proportionality factors to compensate for the variable speed of the hand crank. The tic mark distance of the wave record was used for the corrections. The length of 10 sections of the tic mark was 150 in., from the 240-in. station to the 390-in. station in the wave flume axis. The sequence and values of the coordinates of crest, trough, and tic mark were checked to avoid unreasonable computation results.

The following definitions were employed in this program:

The local wave distance of a wave is defined as a horizontal distance measured from the first tic mark to the mid-point between the crest and the trough. The local wave height of the wave is defined as a vertical distance between the crest and the trough. As a result, each wave in the wave envelope was transformed to a line whose vertical length is the local wave height, and whose horizontal coordinate is the local wave distance. A mean wave height is defined as an arithmetic average value of the local wave height of the entire wave envelope. A deviation wave height is defined as a difference between a local wave height and the mean wave height. A running mean is defined as an average of the deviation wave height over one deviation wave length; however, one-half deviation wave length is used at the end section where the length of envelope is less than one deviation wave length. (The deviation wave length is equal to one-half wave length.) For a sinusoidal curve, the running mean is zero due to its odd function characteristics over one wave length. The deviation wave heights are corrected with the values of the running mean;

that is, deviation wave height minus running mean. The values of the local wave distances and the corrected deviation wave heights of the deviation waves were punched out for the input data of WHVTC2.

The program WHVTC2 computes the best fit sine curve of the equation,

$$y = a \sin (mx+b) + c$$

where y = calculated deviation wave height,

x = local wave distance,

a = amplitude of the best fit sine curve,

m = wave number,

b = phase angle, and

c = best fit mean.

The amplitude of the best fit sine curve, wave number, and phase angle are initialized for the estimate. The more accurate the estimation of the parameters is, the fewer iterations are required, and the greater the probability that the final results will be meaningful. These procedures are accomplished by using a nonlinear curve fitting technique developed by Marquardt (22). The results are plotted by a CalComp Pen Plotter on a finished graph of data points and the best fit sine curve to check the results visually. The reflection coefficient is defined as the ratio of the amplitude of the best fit sine curve to the mean wave height, given as

$$R = a/Hm$$

where Hm = mean wave height.

Fig. 5 shows the processed results of the wave record as shown in Fig. 4:

$$a = 1.035 \text{ in.},$$

$$Hm = 2.40 \text{ in.},$$

$$b = 21.1^\circ, \text{ and}$$

$$R = 43.1\%$$

A comparison was made of the CERC method and the envelope method. Fig. 6 shows a regression line for the incident wave height,

$$Y = -0.03 + 1.05X, \text{ with}$$

$$r^2 = 0.97$$

where Y = incident wave height obtained by the CERC method,

X = incident wave height obtained by the envelope method, and

r^2 = coefficient of determination.

As expected for the oval shape of the wave envelope, a little higher value of the wave height was obtained in the CERC method. Fig. 7 shows a regression line for the reflection coefficient,

$$Y = 0.14 + 0.78X, \text{ with}$$

$$r^2 = 0.87$$

where Y = reflection coefficient obtained by the CERC method, and

X = reflection coefficient obtained by the envelope method.

A little lower value of the reflection coefficient was obtained in the CERC method. Using these equations, the two methods can be converted to each other. Furthermore, the reflected wave height and the incident wave height in the envelope method correspond to the amplitude of the best fit sine curve and the mean wave height in the CERC method, respectively. Another comparison of these two methods shows that the envelope method, which is mathematically oriented, is a simple, easily calculated technique whereas the CERC method, which is statistically oriented, is difficult to calculate unless one has access to the computer programs, WHVTCN and WHVTC2. In any case, the CERC method is more applicable for the correction of spatial wave height variability that occurs in the wave channel. However, the substantial ideas included in both methods are based on the assumption of sinusoidal wave form.

STANDING WAVE THEORY

When a wave meets a barrier, one part of the wave energy is dissipated by breaking, bottom friction, etc., and the remaining part is reflected from the barrier, either partially or totally. The reflected wave travels in the opposite direction of the incident wave, forming a standing wave, or clapotis.

Standing wave theory is divided into linear standing wave theory (first order standing wave theory), and nonlinear standing wave theory (higher order standing wave theory). The linear standing wave was obtained by superposition of two simple harmonic wave functions; whereas, the nonlinear standing wave was obtained by a higher order series expansion of the velocity potential of Stokes' wave theory. Second order standing wave theory is included in the nonlinear standing wave theory. The linear standing wave theory permits simpler calculations and operations, and was therefore used in this study.

The wave motion is considered by Lamb (18) as a potential flow which satisfies the equation of continuity,

$$\frac{\partial^2 \phi}{\partial x^2} + \frac{\partial^2 \phi}{\partial y^2} = 0$$

First Order Standing Wave

The linearized velocity potential of the incident wave is given as

$$\phi i = -\frac{kH}{2m} \frac{\cosh m(d+y)}{\sinh md} \sin (kt-mx)$$

and that of the reflecting wave is given as

$$\phi r = \frac{R\ kH}{2m} \frac{\cosh m(d+y)}{\sinh md} \sin (kt+mx)$$

Thus, the linearized velocity potential for the standing wave can be obtained by superposition of the two components of the velocity potential of the waves,

$$\phi = \phi i + \phi r$$

$$= \frac{kH}{2m} \frac{\cosh m(d+y)}{\sinh md} [(1+R) \cos kt \sin mx -$$

$$(1-R) \sin kt \cos mx]$$

The horizontal component of water particle velocity is

$$u = \frac{kH}{2} \frac{\cosh m(d+y)}{\sinh md} [(1+R) \cos kt \cos mx +$$

$$(1-R) \sin kt \sin mx]$$

The vertical component of water particle velocity is

$$v = \frac{kH}{2} \frac{\sinh m(d+y)}{\sinh md} [(1+R) \cos kt \sin mx -$$

$$(1-R) \sin kt \cos mx]$$

The free water surface profile in Eulerian coordinates is

$$\eta = \frac{H}{2} [(1+R) \sin kt \sin mx + (1-R) \cos kt \cos mx]$$

Second Order Standing Wave

The second order velocity potential for the standing wave was derived by Miche (23), Carry (2), and Rundgren (30) in a slightly different form.

The velocity potential, according to Miche, is given as

$$\phi = \frac{H}{2} \frac{k}{m} \frac{\cosh m(d+y)}{\sinh md} \sin mx \cos kt -$$

$$\frac{3}{16} kH^2 \frac{\cosh 2m(d+y)}{\sinh^4 md} \cos 2mx \sin 2kt$$

Miche developed a theory for the second order of approximations for the standing waves in front of a vertical wall. Rundgren further developed Miche's pure standing wave to the partial standing wave. The velocity potential for the partial standing wave is

$$\phi = \frac{Hk}{2m} \frac{\cosh m(d+y)}{\sinh md} [(1+R) \cos kt \sin mx -$$

$$(1-R) \sin kt \cos mx] - \frac{3}{32} kH^2 \frac{\cosh 2m(d+y)}{\sinh^4 md}$$

$$[(1+R^2) \sin 2kt \cos 2mx - (1-R^2) \cos 2kt \sin 2mx]$$

The horizontal component of water particle velocity is

$$u = \frac{Hk}{2} \frac{\cosh m(d+y)}{\sinh md} [(1+R) \cos kt \cos mx +$$

$$(1-R) \sin kt \sin mx] + \frac{3 mkH^2}{16} \frac{\cosh 2m(d+y)}{\sinh^4 md}$$

$$[(1+R^2) \sin 2kt \sin 2mx + (1-R^2) \cos 2kt \cos 2mx]$$

The vertical component of water particle velocity is

$$v = \frac{Hk}{2} \frac{\sinh m(d+y)}{\sinh md} [(1+R) \cos kt \sin mx - (1-R) \sin kt \cos mx] - \frac{3\, mkH^2}{16} \frac{\sinh 2m(d+y)}{\sinh^4 md} [(1+R^2) \sin 2kt \cos 2mx - (1-R^2) \cos 2kt \sin 2mx]$$

The free water surface profile in the Eulerian coordinates is

$$\eta = \frac{H}{2} [(1+R) \sin kt \sin mx + (1-R) \cos kt \cos mx] - \frac{mH^2}{8} \coth md \{(1+R)^2 [\cos^2 kt - \frac{3 \cos 2kt - \tanh^2 md}{4 \sinh^2 md}] \cos 2mx - (1-R)^2 [\cos^2 kt + \frac{3 \cos 2kt - \tanh^2 md}{4 \sinh^2 md}] \cos 2mx - (1-R^2) [1 + \frac{3}{2 \sinh^2 md}] \sin 2kt \sin 2mx\}$$

Comparison of First and Second Order Standing Wave

A comparison was made between the envelopes created by the first order standing waves with those of the second order standing waves. Using the above equations, the envelopes of wave surface profiles, η, the horizontal particle velocity component, u, and the vertical particle velocity component, v, at designated points on the free water surface were drawn with a CalComp Pen Plotter. The values of reflection coefficient used were R = 0% (Fig. 8), R = 43% (Fig. 9), and R = 100% (Fig. 10), respectively. The wave dimensions for the incident waves were: wave length L = 35 in.; wave height H = 2.4 in; and wave period T = 0.8 sec.

In summary these figures show:

(1) The surface profile envelopes for the first order waves were symmetrical about the horizontal axis. However, those for the second order waves were not symmetrical about the horizontal axis. The asymmetry of the profile envelopes increased as the reflection coefficient increased. The crest envelope height was greater than trough envelope height. The ratio of the crest to trough envelope height changed from 1.4 to 1.75 while the reflection coefficient varied from R = 0% to R = 100%, respectively. The distorted shape of the envelope for the second order waves (Fig. 9) was closer to the actual surface profile envelope (Fig. 4). For the pure standing waves, the surface profiles at the node points were zero. For the progressive waves, no change in the surface profile envelopes was observed for the first and second order waves.

(2) The horizontal velocity envelopes for the first and second order waves were 90° out of phase with those of surface profile envelopes. The maximum and minimum horizontal velocity components occurred at the node and loop points of the surface profile envelopes, respectively. For the pure standing waves, the horizontal velocity at the loop points was zero. For the progressive waves, no change of the horizontal velocity envelopes was observed for the first and second order waves.

For the first order waves, the horizontal velocity component envelopes were not symmetrical about the horizontal axis, even though the surface profile envelopes were symmetrical about the horizontal

axis. The horizontal velocity at the wave crest was greater than that at the wave trough. The difference, according to Wiegel (40), is due to the Eulerian coordinate system. In the Lagrangian coordinate system, the envelopes will be symmetrical about the horizontal axis. For the second order waves, the asymmetrical shape of the envelopes was due to mass transport velocity as expected in the higher order wave theory.

(3) The vertical velocity envelopes for the first and second order waves were in phase with those of surface profile envelopes and were symmetrical about the horizontal axis. The maximum and minimum vertical component occurred at the loop and node points of the surface profile envelopes, respectively. For the pure standing waves, the vertical velocity at the node was zero. For the progressive waves, no change of the vertical velocity envelopes was observed for the first and the second order waves.

The introduction of the reflected waves to the incident progressive waves produced a change, node and loop formation, in the envelope for wave profile and velocity. The reflection coefficient was approximately proportional to the ratio of the particle velocity components of the incident and reflected waves. As a result, the reflection coefficient had more effect on the beach profile change as far as the particle velocity and wave height are concerned.

As mentioned before, some shape differences were found between the wave surface profile for the first order and second order waves. However, the pattern and magnitude of the velocity components were

approximately the same. The wave surface profile is also approximately the same as far as the wave height is concerned. Hence, use of the linear theory can be justified in this study.

WAVES IN SHALLOW WATER

Wave Transformation

As deep water waves travel into shallow water, their characteristics change. When the water depth is approximately one half of the wave length, the waves "feel" bottom. The wave length shortens, the wave celerity slows, and after some small decrease, the wave height increases. When the water depth is about the same as the wave height, the waves break. Most of the wave energy is dissipated in breaking and surging forward to the beach.

Healy (10) explains how the wave energy in deep water is transformed or dissipated in shallow water: friction loss from deep water to surf zone, turbulent loss in the breaker, friction loss in postbreaker uprush, potential energy of inshore water level, friction loss in return flow, and reflected wave energy. For flat slopes, the turbulent loss in the breaker is the main cause of energy dissipation; for steep slopes, the reflected wave energy is most important.

Deep water waves are propagated by orbital motion. The particle motion on the surface makes a circular orbit. The diameter of the orbit is the same as the wave height on the surface, and decreases exponentially with the depth of water. Finally, the orbital motion vanishes at a depth of about one half of the wave length. Thus, the orbital motion does not affect the bottom in deep water and no beach profile occurs.

As the water depth decreases, the particle motion on the surface forms an elliptical orbit with a horizontal major axis. The size of the orbit decreases somewhat, but not exponentially as in the deep water. The orbital motion, with almost the same size of orbits, influences particles on the bottom. As a result, the hydrodynamic force due to the orbital motion will easily initiate particle movement, depending on the grain size of the bottom materials.

The orbital motion of shallow water wave changes the beach profile. But even bigger changes occur after wave breaking. The oscillatory form of the wave motion becomes translatory form, moving particles forward in a single direction. Hence, the breaking wave is important to beach profile change.

Breaking Wave

The phenomena associated with a wave breaking on a beach have long attracted numerous investigators. Very little has been known, however, about the nature of wave breaking. Mathematical expressions of the motion of the water particles do not describe the process of wave breaking itself. Nevertheless, some theoretical and empirical relationships between water depth, wave period, wave height, and beach slope have been derived.

A breaking wave is defined as the highest possible wave at the breaking zone. Using this definition, Stokes (36) deduced that the enclosing crest angle of the highest possible oscillatory wave was 120°. The maximum steepness of the breaking wave, according to

Michell (25) and Havelock (9) for a deep water oscillatory wave, is $H_o/L_o = 0.142$. Gaillard (5) says the maximum steepness for a shallow water wave is H/L = 0.11, while Miche (23) finds it to be H/L = 0.142 tanh (2 d/L). Danel (4) in laboratory tests verified these results. The maximum wave steepness for a progressive wave is 0.142, and the maximum wave steepness for a pure standing wave is 0.218. (The maximum wave steepness for a progressive wave associated with the pure standing wave is 0.109). According to Rankine (29), the wave breaking occurs when the particle velocity at the wave crest reaches the velocity of wave celerity. McCowan (20) assumed that the wave form in the area of the beach was that of a solitary wave. For the solitary wave of maximum height, the ratio of the solitary wave height to the water depth was shown by McCowan (21) to be 0.78. The values obtained by some other investigators have ranged from 0.73 to 1.03.

Galvin (6) performed a laboratory study on breaker types for sloping beaches in order to investigate a relationship between breaker type, wave, and beach slope. Patrick and Wiegel (28) classified breaker types qualitatively as spilling, plunging, and surging. Onshore and offshore quantitative parameters can be shown empirically under different conditions of wave period, wave steepness, and beach slope.

Mass Transport

Under an oscillatory wave, water particle motion is not like

that of unidirectional current flow. Moreover, the trajectories of the water particle are circular in deep water, and elliptical (with their major axes horizontal) in shallow water. The orbital motion is open in higher order theory and is closed in linear theory. The open orbital motion moves the particle forward in the direction of the wave propagation. The actual forward particle motion associated with each wave is termed net drift.

Under the progressive wave, the movement varies with the water depth and the wave characteristics. For large relative depth, such as $d/L = 0.16$, mass transport velocity is in the direction of wave advance at the surface and the bottom, and in the opposite direction at the mid-depth. For small relative depth, such as $d/L = 0.08$, there is a strong forward velocity profile at the bottom, and a reverse velocity profile at the surface. These profiles are derived theoretically by Longuet-Higgins (19) as a conduction solution. Laboratory experiments made by Russell and Osorio (32) presented results which showed that the motion varied with relative depth, but the flow pattern for a given relative depth did not agree with the theoretical results.

In the surf zone, the wave characteristics resemble those of a solitary wave. The illustration by Munk (27) gives an application of the solitary wave theory to the surf zone. He considered that the magnitude and direction of net drift is the resultant of the water particle trajectory of the solitary wave, the return flow, and a slight drift. Field studies conducted by Grant (8) confirmed that

differential velocity affects the transportation of the sand and settling rate. Moreover, the rip currents produced by translatory waves carry particles to the offshore zone.

EXPERIMENTAL EQUIPMENT AND PROCEDURE

Apparatus

The experiments were conducted at the Hydromechanics Laboratories, Texas A&M University, College Station, Texas.

The wave flume (Fig. 11) used for the experiments was 40 ft. long, 8 in. wide and 18 in. deep with flume walls of 3/8 in. plexiglass panels allowing observation of waves over the entire length of the flume.

The wave generating section consisted of a wave paddle, wave filters, and wave absorbers. The wave paddle, piston-type, was a vertical plexiglass plate, and generated monochromatic waves. The wave filters were placed in front of the wave paddle to attenuate multiple reflection, and to improve the wave profile. The filters consisted of a set of corrugated wire meshes and perforated aluminum plates spaced one half in. uniformly in vertical planes parallel to the direction of wave propagation. The absorbers were placed behind the wave paddle to eliminate the dynamic loading on the paddle caused by wave reflection in the confined space between the paddle and the end of the wave tank. The wave absorbers were composed of corrugated wire mesh with a layer of rubberized horse hair on the inclined plexiglass bottom. The clearance between the wall and the paddle plate was sealed by using a petroleum base sealant to minimize leakage around the paddle. The wave generator was attached eccentrically by a rod to a rectangular driving plate driven by a variable

speed motor (3 HP).

The wave envelope was recorded by using a capacitance type wave probe connected to a Hewlett Packard Dual Channel Carrier Amplifier Recorder (Model No. 321). The wave probe was attached to a carriage. The carriage was drawn from the 240-in. station to the 390-in. station at the speed of 3 in./sec. by a hand crank. The calibration of the wave probe was linear, and was obtained by raising and lowering the wave probe in still water before each measurement.

A wheel with a diameter of 4.7 in. was used to record tic marks on the wave profile record by completing an electric-circuit and causing a marker pen to record. At a point on the periphery of the wheel, an electric contact completed the circuit each time when it came in contact with the track on which the carriage moved. By measurement of the distance of two subsequent tic marks, one was able to check the linearity of the carriage cranking speed.

The wave period was varied by the speed control lever, and was determined by timing with an electric stop watch the number of strokes the wave paddle generated. The wave height was changed by varying the eccentricity of the rectangular driving plate.

A model beach with a slope of 1/30 was erected at the section from the far end of the flume to the 240-in. station. Significant points of the deformed beach were taken by visual readings from a grid system on one side of the flume wall. The sand used for the experiments was natural beach sand having a median diameter, d_{50},

of about 0.17 mm. All sand used was collected on the beach of Matagorda Peninsula, Texas.

Procedure

Two kinds of tests, a natural beach test and a seawall beach test, were conducted. To study the effect of wave heights and wave periods on the beach profile, ten sets of wave characteristics for each of these conditions were run in the natural beach test. Measurements were made of the wave period, wave profile envelope, wave breaking height, wave breaking point, and the change of the beach profile. To study seawall position relative to the wave breaking point, three sets of wall characteristics for each of the above ten conditions were run in the seawall beach test. Measurements were made of the wave period, wave profile envelope, seawall distance, and the change of the beach profile.

For the natural beach test, the initial beach profile was molded along a reference line with a slope of 1/30. The wave paddle stroke and speed were kept constant for each run which consisted of one natural beach test and three seawall beach tests. The still water depth of 8 in. was also kept constant; there was, therefore, no consideration in these experiments of tidal change, such as would be the case on an actual beach. The sloping beach face was allowed to change for a period of 48 hours. Generally, the beach became stable at the end of this time period. The final beach profile was marked on the flume wall and was used as a reference line for

remolding in the subsequent seawall tests.

A seawall, simulated by an aluminum plate 1/8 in. thick, was erected at the final wave breaking point on the deformed natural beach. The seawall test following the natural beach test was then continued for 24 hours using the same wave period and paddle stroke. At the completion of this test period, the previous final beach was remolded for the next seawall beach test. The seawall was placed at the points of 1.00, 0.75, and 0.50 Xb, respectively. (Xb is the distance from the original shoreline to a point where waves break on a natural beach after a 48-hour run.) Three wave periods, 0.8, 1.0, and 1.3 sec., and three paddle strokes, 0.7, 1.1, and 1.5 in., produced nine wave heights. Later, a tenth wave was formed from a wave period of 0.8 sec., and a paddle stroke of 1.9 in.

Generally speaking, the wave height and wave length generated were governed by the wave period, paddle stroke, and water depth. The wave length, L, was very close to the value calculated from linear wave theory, given as $L = gT^2/2\pi \tanh(2\pi d/L)$. However, the equation of the wave height was not available for the particular wave channel. Qualitatively, the wave height generated as a function of the paddle stroke and wave period in a constant water depth. On the basis of the laboratory measurements, a regression equation was obtained by using a multiple linear regression analysis computer program. The equation can be expressed as

$$H = 0.66 + 1.14 \text{ (paddle stroke)} - 0.48 \text{ (wave period)}, \text{ with}$$

$$r^2 = 0.86$$

OBSERVATION

Sand Movement

As soon as the first few waves passed, a series of ripples and sand particle suspension were observed on the bed surface near the point of breaking wave. As the wave action progressed, the ripple formation developed, first in the inshore zone and then in the offshore zone (Fig. 12). The shape of the ripples was regular in the offshore zone, but irregular in the inshore zone because of the violence of the wave breaking. The size of the ripples on the sand bar crest was larger than that on the sand bar trough. The ripples formed along the whole bed surface under the maximum wave height. But under the minimum wave height, the ripple formation was limited to the inshore zone during the entire run, thus demonstrating that ripple formation is a function of wave height and water depth.

As the ripples grew, more sand particles were continuously suspended, moving back and forth. After a several hour time duration, considerable erosion had occurred in the original uniform sloping beach profile in the inshore zone. A portion of the eroded sand was moved to the beach to form a berm, and the other portion was moved to the offshore zone to form a series of bars. However, there was very little change of the beach profile around the wave breaking point.

In deep water, the horizontal particle velocity under the crest (forward direction) and that under the trough (backward direction)

are equal in magnitude. In shallow water, however, the horizontal particle velocity under the crest is greater than that under the trough. Laboratory tests made by Morison and Crooke (26) showed that the horizontal particle velocity under the crest is about twice as much as that under the trough. After wave breaking, the wave with increased forward velocity, rushed up the beach face until it completely lost its kinetic energy. Some of the water percolated down through the sand surface leaving a part of the transported sand on the beach surface; the remaining part flowed down to the swash zone. In this manner, the berm was built to the height of the wave uprush peak point. Long period waves kept the ground water table lower than short period waves, because of a longer interval between waves. Consequently, the long period waves generated the berm type of beach profile rather than the bar type of beach profile.

The larger forward velocity raised the water surface in the swash zone. To maintain the water balance, some of the water flow moved in the opposite direction of the wave propagation. This is one of the reasons for wave induced current formation in the littoral zone. Field studies made by Grant (8) confirmed the mass transport of water to the offshore zone. The wave induced current carried a part of the suspended sand until the flow was neutralized by the forward velocity due to wave action. At this point, the sand particles settled down to form a bar. As the bar formation progressed, a considerable amount of change in the reflection coefficient occurred.

A comparison was made to observe the effect of seawall distance on sand movement of the beach. Four seawall distances were compared with respect to the wave breaking distance on the uniform sloping beach, 1/30. The seawall distances used were 1.50, 1.00, 0.75, and 0.50Xb, respectively. For the case of the nonbreaking wave, 1.5 and 1.0Xb, the sand movement was confined to the two subsequent loop points, hence, no sand transportation was observed beyond the next loop points. After a 24-hour run, the eroded beach section would be filled up by the deposited sand under the node. However, for the case of the broken wave, 0.75 and 0.50Xb, some sand transportation was observed beyond the loop points. After a 24-hour run, as a result, the eroded section of the beach would not be filled up by the deposited sand under the node points. Some deposits were observed at the down stream section of the beach, showing that the role of wave induced current is important to sand transportation.

Particle Trajectories

The wave induced particle motion consists of two components created by progressive and standing waves. To compare the particle motion of the progressive waves with that of standing waves, a flat beach (1 in. thick) was constructed in the flume from the 240-in. to the 300-in. station.

Two floating Accentulite bulbs, activated by water, were used to show particle motion on the wave surface. Placing the bulbs in water closed an electrical circuit, thus lighting them. The bulbs

were cylindrical, 0.5 in. in diameter, 2.7 in. in length. For buoyancy, a piece of styrofoam was attached to the bulb body. After contact with the water, each bulb would last about one hour.

Trajectories of the bulbs under the progressive waves, T = 0.8 sec., are shown in Fig. 15 for paddle stroke = 1.5 in., and Fig. 16 for paddle stroke = 0.7 in. The direction of net drift was the same as the direction of the wave propagation, from right to left, creating a series of open, elliptical orbits with horizontal major axes. As shown in Fig. 8, neither node nor loop point was formed in the envelope of surface profile for the progressive wave. The straight envelope of the trajectories showed that the reflection was negligibly small in this case.

Trajectories of the bulbs for the pure standing waves, T = 0.8 sec., are shown in Fig. 17 for paddle stroke = 1.5 in., and Fig. 18 for paddle stroke = 0.7 in., respectively. The standing waves were generated by erecting a vertical seawall at the 240-in. station. However, no unidirectional motion was observed, as had occurred for the progressive waves. The motion of the particles and the height of the wave envelope varied between node and loop. The motion at the loop point is vertical, and the height of the wave envelope is maximum, whereas the motion at the node point is horizontal, and the height of the envelope is minimum.

A series of pictures taken by Wallet and Ruellan (39) shows the particle motions as they vary from progressive waves to pure standing waves. Under the progressive wave condition, the orbits are ellipses

with their major axes horizontal. Under the standing wave conditions, the orbits are ellipses, but the directions of their major axes are different; that is, horizontal at the node where the horizontal motion is maximum, and vertical at the loop where the vertical motion is maximum. With an increase of the reflection coefficient, the eccentricity of the elliptical orbits increases, and finally a set of curves with vertical asymptotes is formed by the pure standing waves.

An attempt was made to compare beach profile changes under a progressive wave and a standing wave. A flat beach was constructed in the nonbreaking wave section to eliminate the effect of wave transformation due to sloping beach and wave breaking on the beach. For the standing wave (Fig. 15), the flat beach was deformed as shown in Fig. 17 after a 24-hour duration. Deposition occurred at the bottom under the node. At the bottom under the loop, however, the beach remained plane without ripples. This shows that the horizontal velocity component, insofar as the sand particle movement is concerned, is a more predominant factor than the vertical velocity component. The vertical velocity component keeps the sand particles in suspension, and the horizontal velocity component transports the sand particles to the node and deposits them there. The direction of particle movement on the wave surface, as shown in Fig. 15, is from node to loop. However, the direction of sand particle movement on the bed surface, as shown in Fig. 17, is from loop to node. The two opposite directions of the flow make a closed circulation between the node and the loop. For the progressive wave (Fig. 13), a series

of regular size ripples covered the whole bed without considerable change of beach profile. The different type of particle motion caused the different type of beach scour pattern between the progressive wave and the standing wave.

Problems

The following problems were encountered during laboratory tests:

(1) The wave profile envelope, recorded for long period waves, T = 1.3 sec., revealed a series of minor waves propagating independently at different speeds. Galvin (7) pointed out that finite amplitude, periodic, sinusoidal waves generated in shallow water of constant depth divided into two or more unbroken waves, i.e. solitons. The solitons travel at speeds dependent on their height. When a large soliton overtakes a small one, it decreases in wave height while it is superimposed on the small one and increases in wave height after it has passed the small one. As far as the wave height is concerned, some correction may be necessary. It is not known quantitatively what the effect of the solitons is on the standing wave envelope.

(2) The mean wave height varied with duration, even though both motor speed and paddle stroke were kept constant during each test run. However, no attempt was made to eliminate the temporal wave height variability. Actually, it was extremely difficult to maintain a constant wave height throughout the entire run.

RESULTS

Natural Beach Test

The reflection from the initial beach slope of 1/30 was negligibly small regardless of wave conditions. The reflection coefficient was less than 5%. As shown in Fig. 18, short period waves, T = 0.8 sec., gave a higher value of reflection coefficient than long period waves, T = 1.0 sec. The initial maximum value of the reflection coefficient was usually reached within 24 hours, and the peak coincided with the time of berm and bar formation on the beach, thus stabilizing the beach profile. After that, the reflection coefficient changed only slightly during the remaining hours of the test run. These results demonstrate that beach profile change is a main factor of reflection coefficient change, even though that relationship is difficult to explain quantitatively.

Apparently, certain relationships exist between the water wave and the sand wave formation. The average distance between the sand bar generated was very close to one-half local wave length; that is, 2.0 ft. for T = 1.3 sec., 1.5 ft. for T = 1.0 sec., and 1.0 ft. for T = 0.8 sec., respectively. It appears that these relationships hold for a sloping as well as a flat beach. The height of the sand bar was also proportional to the incident wave height. Fig. 19 shows the relationship between sand bar steepness in the nonbreaking zone and the incident wave steepness in deep water. The relationship correlated well with the reflection coefficient: a high value of the

reflection coefficient enhanced the sand bar steepness.

In the berm formation, the wave period was also a predominant factor. A comparison was made of the berm size under 48-hour duration and different wave heights, Fig. 20 for T = 1.3 sec., and Fig. 21 for T = 0.8 sec. These figures show that on the berm formation the wave height had little effect, but the wave period was affected significantly. The berm, having a slope of 1/4, was formed within 2.0 ft. from the original still water line. The slope was affected slightly by the wave conditions. The reflection from the berm was small, since most of the wave energy was dissipated in the form of wave breaking and uprush. Consequently, the reflection coefficient is negligible in creating the berm formation.

The sand eroded in the inshore zone by the wave breaking was transported shoreward to form a berm and seaward to form a series of bars. Fig. 22 shows a relationship between the berm cross section area and the erosion cross section area under the different values of deep water wave steepness. Waves of low steepness moved sand to the shoreline from the erosion area; whereas, waves of the high steepness moved sand to the offshore zone from the erosion area. Generally, these results coincide with studies by Johnson (16) on wave steepness for summer profile (swell or berm type), and winter profile (storm or bar type).

The maximum ultimate scour depth of the natural beach occurred in the inshore zone. The scour depth was less than the breaking wave height (Fig. 23). This means that the breaking wave height can be

used to predict the scour depth on the natural beach. A regression analysis was conducted to obtain a regression equation for 10 observations (48-hour duration):

$$S = 0.544\ Hb^{1.29}, \text{ with}$$

$$r^2 = 0.80$$

where S = maximum ultimate scour depth, and

Hb = breaking wave height.

Seawall Beach Test

A seawall erected on the stabilized natural beach changed the reflection coefficient as well as the pattern of the beach profile. The reflection came from both the seawall and the beach. It was also found that the reflection from the stabilized beach was considerable for most cases of the natural beach test.

Generally, the values of the reflection coefficient for long period waves, T = 1.3 sec., were smaller than those for short period waves, T = 0.8 sec. As a result, the low steepness wave provided the low reflection coefficient as shown in Table 2, Appendix D.

The reflection coefficient for the breaking waves was usually higher than that of broken waves (Fig. 24). The energy dissipated after wave breaking was used to increase the scour depth at the toe of the seawall. Hence, low reflection coefficients corresponded to deep scour depths (Fig. 25). The effect of the relative seawall distance or the stabilized natural beach (Fig. 26) is shown in Fig. 27 for X/Xb = 1.00, Fig. 28 for X/Xb = 0.75, and Fig. 29 for X/Xb = 0.50.

There were some changes in the location and shape of the sand bar trough. When the seawall was placed on the bar trough, the standing wave made deeper troughs, but the crests of the sand bar were almost the same. Addition of the seawall changed the nature of the standing wave, which resulted in an increase in particle velocity. This increase was strong enough to disturb the sand particles on the bar trough. When the seawall was placed on the bar crest, the profile pattern was completely changed; the previous bar crest became the bar trough and vice versa. The trend was very clear during tests using the long period wave, T = 1.3 sec. The point of node envelope and bar crest approximately coincided with a slight phase shift.

The maximum ultimate scour depths at the toe of seawalls were found between X/Xb = 0.75 and X/Xb = 0.50. At a value of X/Xb = 1.00, the minimum ultimate scour depth occurred (Fig. 30). (X/Xb is relative seawall distance.)

Regression Analysis

As seen before, many variables are related to the scour phenomenon in front of a seawall due to wave action. But the variables, in general, can be classified in three categories, each of which contains variables: wave, beach, and seawall. The variables of wave criterion are wave period, T, deep water incident wave height, Ho, deep water standing wave height, Hs, breaking wave distance from the original shoreline, Xb, and acceleration of gravity, g. The variables of beach criterion are scour depth, S, and beach slope, θ. The

variables of the seawall criterion are seawall distance from the original shoreline, X, and seawall inclination angle, α. However, the reflection coefficient was not considered as a variable. In a standing wave system, the reflection coefficient indicates only the degree of reflecting capacity of an incident wave from a barrier. Moreover, the feature of the scour depth is primarily related to the dimension of the waves acting on the beach. Hence, the standing wave height is considered as a variable.

Additional variables to be considered are the specific gravities of water and sand, the median grain size of sand, etc. In this study, the following variables were kept constant: specific gravity of water, 1.00; specific gravity of sand, 2.65; median grain size of sand, 0.17 mm; beach slope, 1/30; and seawall inclination angle, 90°.

Through a dimensional analysis, a functional expression including the above variables is possible:

$$f(T,Ho,Hs,Xb,g,S,X) = 0$$

Using these variables, the following dimensionless terms are obtained:

$$f(S/Ho,\ Hs/gT^2,\ X/Xb) = 0$$

Relative scour depth, S/Ho, can be expressed as

$$S/Ho = f(Hs/gT^2,\ X/Xb)$$

Since $Ls = gT^2/2\pi$, the term, Hs/gT^2, can be substituted by Ls. Thus, one may write

$$S/Ho = f(Hs/Ls, X/Xb)$$

In order to obtain a quantitative relationship of these variables, three types of regression models were set up and compared with the value of multiple coefficient of determination, r^2. The three regression models used for this study were arithmetic, semilogarithmic, and logarithmic.

The computer program used for the regression analysis was Maxi-MLR, 1971 revised edition of The Institute of Statistics at Texas A&M University. The program was intended for easy implementation of regression computations for small data sets (maximum of 20 independent variables and 500 observations) using the resident WATFIV compiler of the IBM 360/65 computer. The program performed a step-down variable selection and a feedback after the selection stops. The t-level for removal was set at 0.05 for these regression analyses.

If the relation of relative scour depth to deep water standing wave steepness and relative seawall distance is assumed to be arithmetic in form, the multiple linear regression relation may be expressed in the form

$$S/Ho = \beta_o + \beta_1(X/Xb) + \beta_2(Hs/Ls)$$

where β_o, β_1, and β_2 are to be calculated by a computer program. A multiple regression analysis of 104 observations gave an equation of the form

$$S/Ho = -2.19 + 1.39(X/Xb) + 12.52(Hs/Ls), \text{ with}$$
$$r^2 = 0.72$$

If the relation is assumed to be semilogarithmic in form, the multiple linear regression relation may be expressed in the form

$$S/Ho = \beta_o + \beta_1 \ln(X/Xb) + \beta_2 \ln(Hs/Ls)$$

A multiple regression analysis of the semilogarithmic model for a total of 104 observations, ranging from 4- to 24-hour duration, gave an equation of the form

$$S/Ho = 1.73 + 0.85\ \ln(X/Xb) + 0.62\ \ln(Hs/Ls), \text{ with}$$
$$r^2 = 0.81$$

For a total of 32 observations, 24-hour duration, the regression equation was

$$S/Ho = 1.95 + 0.57\ \ln(X/Xb) + 0.72\ \ln(Hs/Ls), \text{ with}$$
$$r^2 = 0.84$$

Thus, a slightly higher value of r^2 was obtained.

If the relation is assumed to be logarithmic in form, the multiple linear regression relation may be expressed in the form

$$1 - S/Ho = e^{\beta_o}(X/Xb)^{\beta_1}(Hs/Ls)^{\beta_2}$$

A multiple regression analysis of the logarithmic model for a total of 104 observations gave an equation of the form

$$1 - S/Ho = 0.360(X/Xb)^{-0.67}(Hs/Ls)^{-0.36}, \text{ with}$$

$$r^2 = 0.74$$

The semilogarithmic regression model gave the highest value of $r^2 = 0.84$. Since this model gave the highest correlation, it was used for the result of the regression analysis of the experimental data for the seawall beach test.

On the basis of the above regression equation, one can obtain relative scour depth (S/Ho) as a function of relative seawall distance (X/Xb) and deep water standing wave steepness (Hs/Ls). Fig. 31 shows variations of the relative seawall distance to the deep water standing wave steepness and the relative scour depth. Generally, the relative seawall distance is proportional to the deep water standing wave steepness for the same value of the relative scour depth. For small values of the deep water standing wave steepness ($Hs/Ls < 0.02$), the relative scour depth is nearly independent of the seawall position. For larger values of the deep water standing wave steepness ($Hs/Ls > 0.05$), however, the relative scour depth is dependent upon the seawall position. (For the relative scour depth, negative sign refers to scour, and positive sign refers to deposition.) Using Fig. 31, one can easily predict the scour depth at the toe of a seawall instead of using the regression equation.

CONCLUSIONS AND RECOMMENDATIONS

Conclusions

The following conclusions were drawn in this study:

1. In the calculation of reflection coefficient and incident wave height, the CERC method was a more applicable method for the correction of spatial wave height variability than the envelope method. Both methods, however, were based on the linear wave assumption.

2. The wave surface profile envelope for the second order standing waves gave better correlation to the measured profile envelope than that for the linear waves; however, the envelopes for the components of particle velocity were not much different. Hence, the linear standing wave theory was usable with minimum efforts.

3. The introduction of a seawall changed the wave reflection coefficient as well as the scour depth at the toe of a seawall. A regression equation was obtained by using a multiple linear regression analysis computer program, given as

$$S/Ho = 1.94 + 0.57 \ln(X/Xb) + 0.72 \ln(Hs/Ls), \text{ with}$$
$$r^2 = 0.84$$

The above equation may be used to predict scour depth at the toe of the seawall.

Recommendations

Further studies should investigate the following:

1. The experiments should be repeated, using a wider range of wave type, different sizes of bed sand, different slopes of beach, and seawall inclination angle.

2. The wave height variability is an inherent problem in many wave channels. A method for the correction of the temporal wave height variability should be devised.

3. The relationship between the wave spectrum of irregular waves and the corresponding wave spectrum of sand wave at the bottom by using a spectral analysis should be studied.

4. The scale effect should be investigated by using a different size of flume.

5. The orbital velocity of standing waves with various reflection coefficients should be measured to compare with both first and second order standing waves.

APPENDIX A

APPENDIX A

REFERENCES

1. Ahlquist, J., and James, W., Computer Programs: WHVTCN (720S8R11K0), WHVTC2 (720S8R11Z0), ADP Office, Coastal Engineering Research Center, Washington, D.C., 1971 (unpublished).

2. Carry, C., "Clapotis Partiel", La Houille Blanche, No. 4, September, 1953, pp. 482-494.

3. Chesnutt, C.B., and Schiller, R.E., Jr., "Scour of Simulated Gulf Coast Sand Beaches Due to Wave Action in Front of Sea Walls and Dune Barriers", COE Report No. 139, TAMU-SG-71-207, May, 1971.

4. Danel, P., "On the Limiting Clapotis, Gravity Waves", National Bureau of Standards, Circular 521, 1952, pp. 35-38.

5. Gaillard, D.D., "Wave Action in Relation to Engineering Structures", reported from 1935 ed., The Engineer School, Fort Belvoir, Virginia, 1945.

6. Galvin, C.J., Jr., "Breaker Type Classification on Three Laboratory Beaches", Journal of Geophysical Research, Vol. 73, No. 12, June, 1968, pp. 3651-3659.

7. Galvin, C.J., Jr., "Finite-Amplitude, Shallow Water-Waves of Periodically Recurring Form", Proceedings of Symposium of Longwaves, Newark, Delaware, (in press), 1972.

8. Grant, U.S., "Waves as a Sand Transporting Agent", American Journal of Science, Vol. 241, 1943, pp. 117-123.

9. Havelock, T.H., "Periodic Irrotational Waves of Finite Height", Proceedings of Royal Society of London, Series A 95, 1918, pp. 38-51.

10. Healy, J., "Wave Damping Effect of Beaches", Proceedings of Minnesota International Hydraulic Convention, Minneapolis, Minnesota, 1953, pp. 213-220.

11. Herbich, J.B., Murphy, H.D., and Van Weele, B., "Scour of Flat Sand Beaches Due to Wave Action in Front of Sea Walls", Proceedings of the Santa Barbara Specialty Conference on Coastal Engineering, 1965, pp. 705-726.

12. Herbich, J.B., and Ko, S.C., "Scour of Sand Beaches in Front of Seawalls", Proceedings of the Eleventh Conference on Coastal Engineering, 1968, pp. 622-643.

13. Herbich, J.B., "Comparison of Model and Beach Scour Patterns", Proceedings of the Twelfth Conference on Coastal Engineering, 1970, pp. 1281-1300.

14. Hunt, I.A., Jr., "Design of Sea-Walls and Breakwaters", Transactions of ASCE, Vol. 126, Part IV, 1961, pp. 542-570.

15. Iribarren, R.C., and Casto Nogales Y Olano, "Protection of Ports", Seventeenth Congress of International Association of Navigation Congress, Section 2, Communication 4, Lisbon, Portugal, 1947.

16. Johnson, J.W., "Scale Effects in Hydraulic Models Involving Wave Motion", Transactions American Geographical Union, Vol. 30, 1949, pp. 517-525.

17. Keulegan, G.H., "Report on a Method of Determining the Wave Form of Oscillatory Waves Reflected from a Breakwater", U.S. National Bureau of Standards, July 31, 1950, (unpublished).

18. Lamb, H., Hydrodynamics, 6th ed., Dover Publications, Inc., New York, 1945.

19. Longuet-Higgins, M.S., "Mass Transport in Water Waves", Philosophical Transaction of Royal Society of London, A 245, No. 903, 1953, pp. 535-581.

20. McCowan, J., "On the Solitary Wave", Philosophical Magazine, 5th Series, Vol. 32, 1891, pp. 45-58.

21. McCowan, J., "On the Highest Wave of Permanent Type", Philosophical Magazine, 5th Series, Vol. 38, 1894, pp. 351-358.

22. Marquardt, D.W., "An Algorithm for Least Squares Estimation of Nonlinear Parameters", Journal of the Society for Industrial & Applied Mathematics, Vol. 2, 1963, pp. 431-441.

23. Miche, M., "Undulatory Movement of the Sea", Annales des Ponts et Chaussées, Paris, 1944.

24. Miche, M., "The Reflecting Power of Maritime Works Exposed to Action of the Swell: Annales des Ponts et Chaussées", Abstracts in Bulletin of the Beach Erosion Board, Vol. 7, No. 2, 1951.

25. Michell, J.H., "On the Highest Waves in Water", Philosophical Magazine, Vol. 36, 5th Series, 1893, pp. 430-437.

26. Morison, J.R., and Crooke, R.C., "The Mechanics of Deep Water, Shallow Water, and Breaking Waves", Technical Memorandum, No. 40, Beach Erosion Board, Corps of Engineers, Washington, D.C., 1953.

27. Munk, W.H., "The Solitary Wave and Its Application to Surf Problems", Annuls New York Academy of Science, Vol. 51, 1949, pp. 376-424.

28. Patrick, D.A., and Wiegel, R.L., "Amphibian Tractors in the Surf", Proceedings of the First Conference on Ships and Waves, Council on Wave Research and American Society of Naval Architects and Marine Engineers, 1955.

29. Rankine, W.J., "Summary of Properties of Certain Streamlines", Philosophical Magazine, 4th Series, Vol. 29, 1864, pp. 282-288.

30. Rundgren, L., "Water Wave Forces", Transactions of the Royal Institute of Technology, The Institute of Hydraulics, Bulletin No. 54, Stockholm, Sweden, 1958.

31. Russell, R.C.H., and Inglis, C., "The Influence of a Vertical Wall on a Beach in Front of It", Proceedings of the Minnesota International Hydraulics Convention, Minneapolis, Minnesota, 1953, pp. 221-226.

32. Russell, R.C.H., and Osorio, J.D.C., "An Experimental Investigation of Drift Profiles in a Closed Channel", Proceedings of the Sixth Conference on Coastal Engineering, 1958, pp. 171-183.

33. Sato, S., Tanaka, N., and Irie, I., "Study on Scouring at the Foot of Coastal Structures", Proceedings of the Eleventh Conference on Coastal Engineering, 1968, pp. 579-598.

34. Sawagari, T., "Scouring Due to Wave Action at the Toe of a Permeable Coastal Structure", Proceedings of the Tenth Conference on Coastal Engineering, 1966, pp. 1036-1047.

35. Schoemaker, H.J., and Thijsse, J.Th., "Investigation of the Reflection of Waves", Congress of the Third Meeting of the International Association of Hydraulic Research, Grenoble, 1949.

36. Stokes, G.G., "On the Theory of Oscillatory Waves", Transactions of Cambridge Philosophical Society, Vol. VIII, 1847, p. 441.

37. Ursell, F., Dean, R.G., and Yu, Y.S., "Forced Small-Amplitude Water Waves: A Comparison of Theory and Experiment", Journal of Fluid Mechanics, Vol. 7, Part 1, January, 1960, pp. 33-52.

38. U.S. Army Corps of Engineers, Coastal Engineering Research Center, "Shore Protection, Planning and Design", Technical Report No. 4, 1966, p. 213.

39. Wallet, A., and Ruellan, F., "Trajectories of Particles within a Particle Partial Clapotis", La Houille Blanche, No. 4, 1950, pp. 483-489.

40. Wiegel, R.L., Oceanographical Engineering, Prentice-Hall, Inc., Englewood Cliffs, N.J., 1964, p. 16.

APPENDIX B

APPENDIX B

NOMENCLATURE

The following symbols are used in this paper:

a = amplitude of best fit sine curve;

A_i = amplitude of incident wave;

A_r = amplitude of reflected wave;

d = still water depth;

d_{50} = median diameter of bed material;

E = total wave energy;

E_i = incident wave energy;

E_r = reflected wave energy;

$f( )$ = function of ( );

g = acceleration of gravity;

H = wave height;

H_i = incident wave height;

H_ℓ = wave height at the loop envelope;

H_m = mean wave height;

H_n = wave height at the node envelope;

H_o = deep water wave height;

H_r = reflected wave height;

H_s = deep water standing wave height;

k = wave frequency;

L = local wave length;

L_o = deep water wave length;

m = wave number;

r^2 = coefficient of determination;

R = reflection coefficient;

R′ = theoretical reflection coefficient;

Rx = relative seawall distance;

S = scour depth at the toe of a seawall or scour depth at a particular point along the beach profile without a seawall;

t = duration or time;

T = wave period;

u = horizontal component of particle velocity;

v = vertical component of particle velocity;

x = horizontal coordinate;

X = horizontal distance from the original shoreline;

Xb = horizontal distance from the original shoreline to the point where the wave breaks;

y = vertical coordinate;

α = seawall inclination angle;

γ = unit weight of water;

η = surface profile of standing wave;

ηi = surface profile of incident wave;

$\eta \ell$ = amplitude of the surface profile at loop point;

ηn = amplitude of the surface profile at node point;

ηr = surface profile of reflected wave;

θ = beach slope;

π = 3.14159...;

ρ = intrinsic reflection coefficient;

ϕ = velocity potential;

ϕi = velocity potential of incident wave; and

ϕr = velocity potential of reflected wave.

APPENDIX C

FIGURES

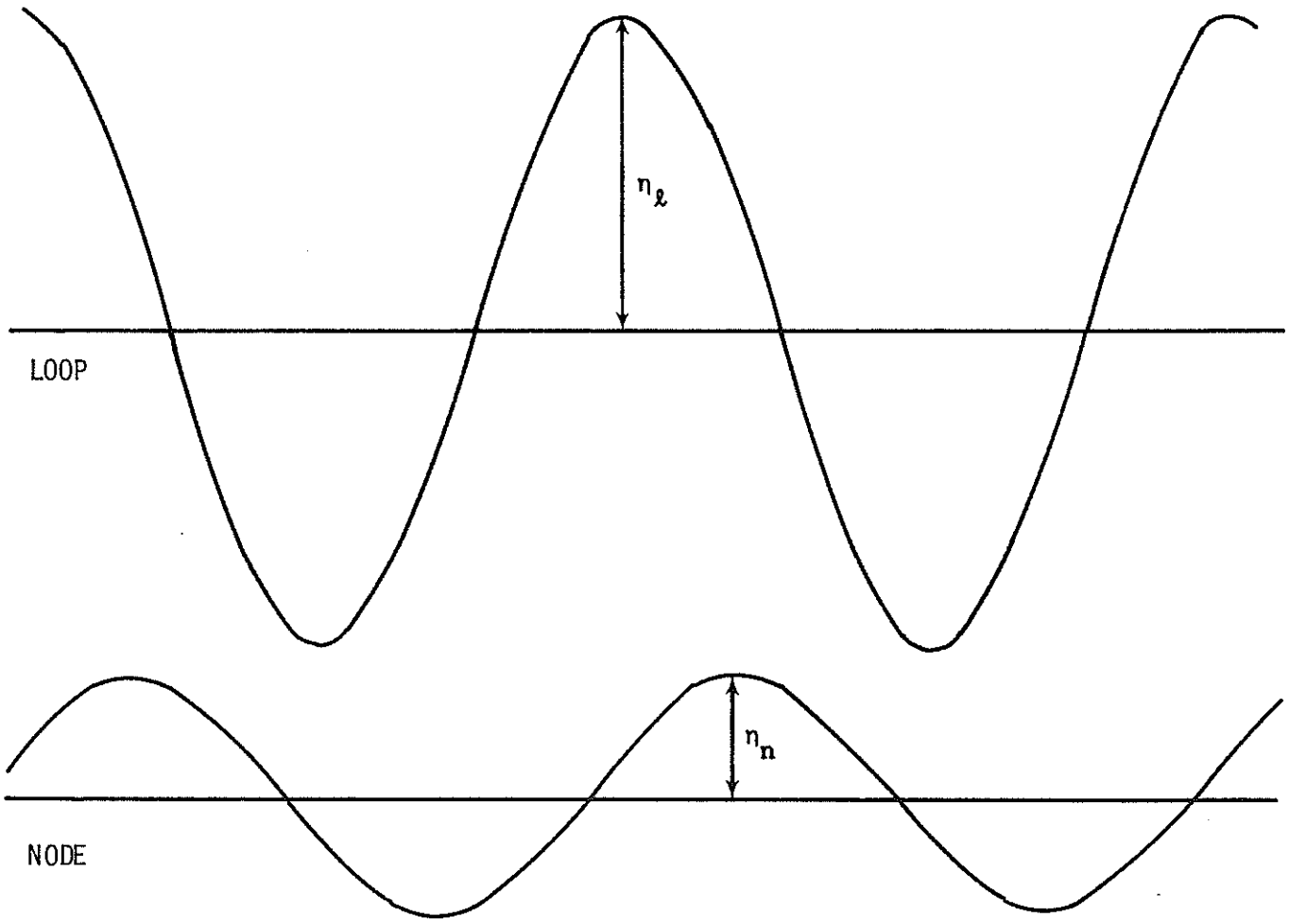

Fig. 1 THE METHOD OF ONE PROBE FOR MEASUREMENT OF THE WAVE PROFILE

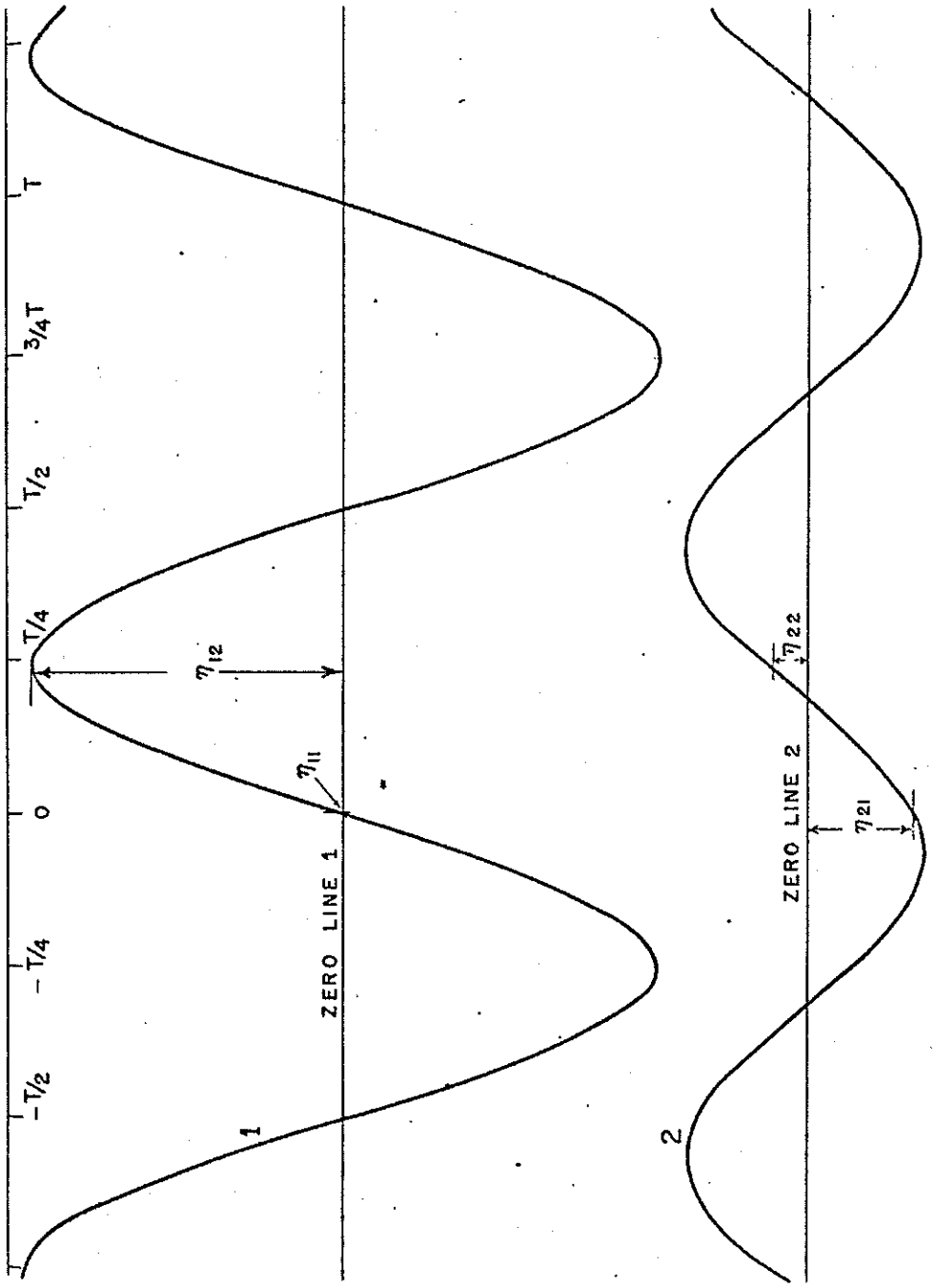

Fig. 2 THE METHOD OF TWO PROBES FOR MEASUREMENT OF THE WAVE PROFILE (AFTER KEULEGAN)

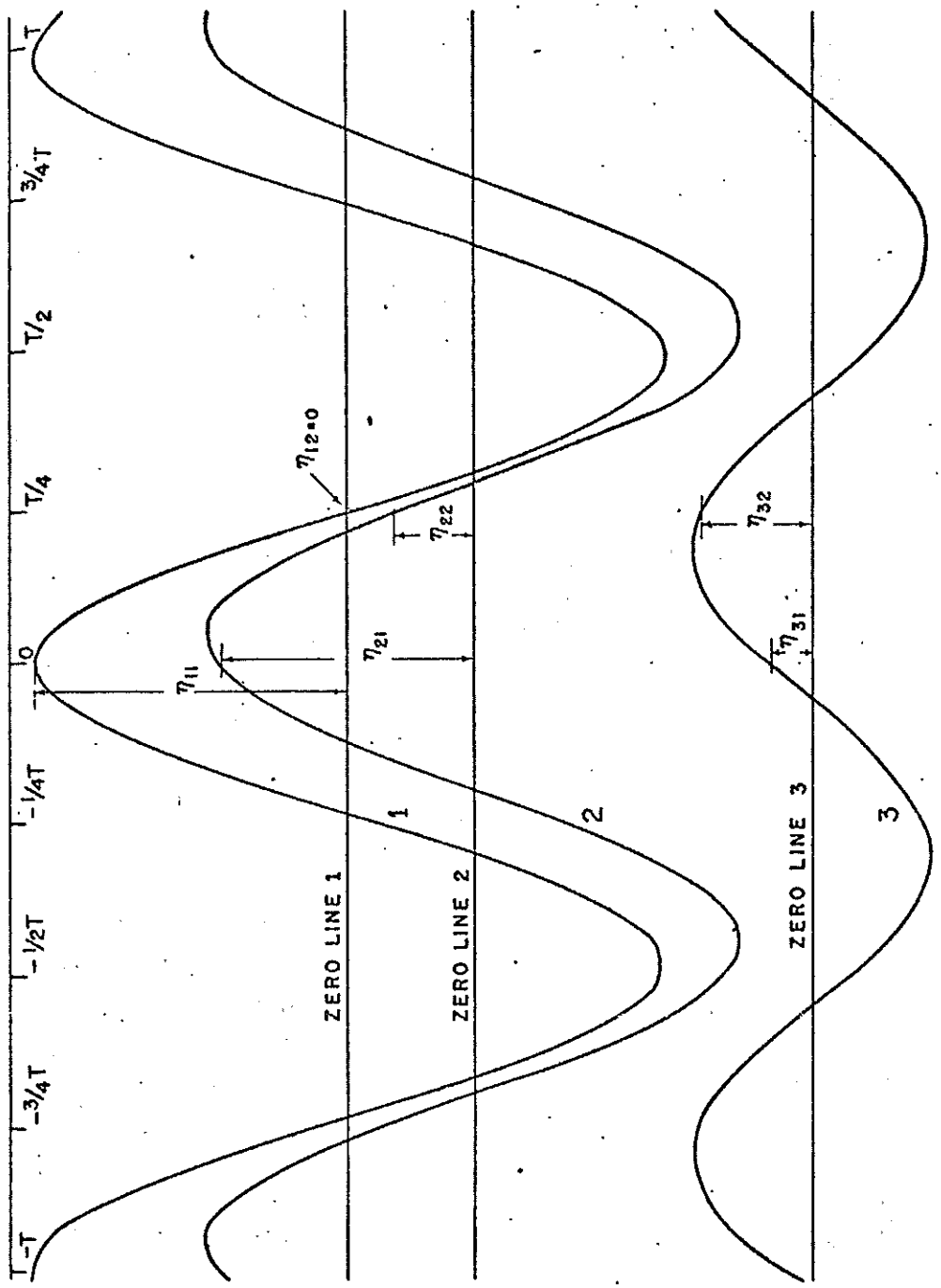

Fig. 3 THE METHOD OF THREE PROBES FOR MEASUREMENT OF THE WAVE PROFILE (AFTER KEULEGAN)

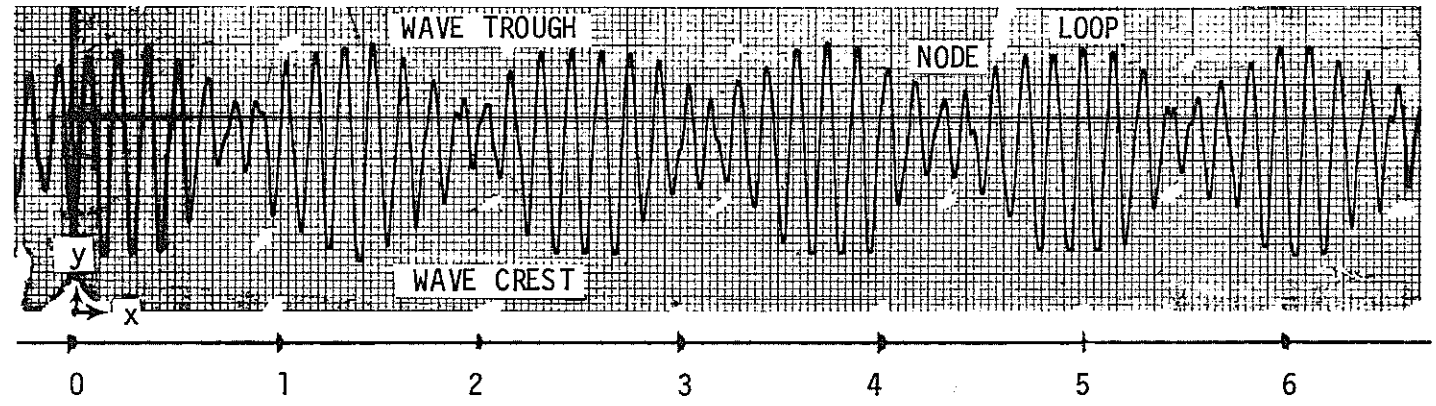

240-IN STATION

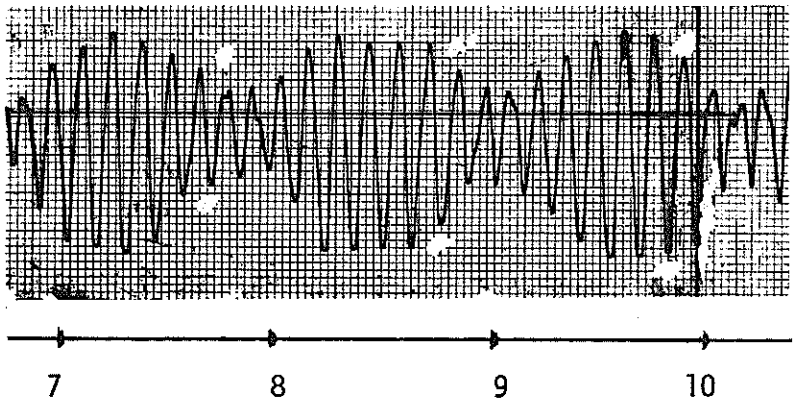

370-IN STATION

WAVE PERIOD : 0.8 SEC
PADDLE STROKE : 1.9 IN
DURATION : 24 HR
REFLECTION COEFFICIENT : 43.1 %
MEAN WAVE HEIGHT : 2.4 IN
RELATIVE SEAWALL DISTANCE : 0.75

Fig. 4 WAVE ENVELOPE RECORD

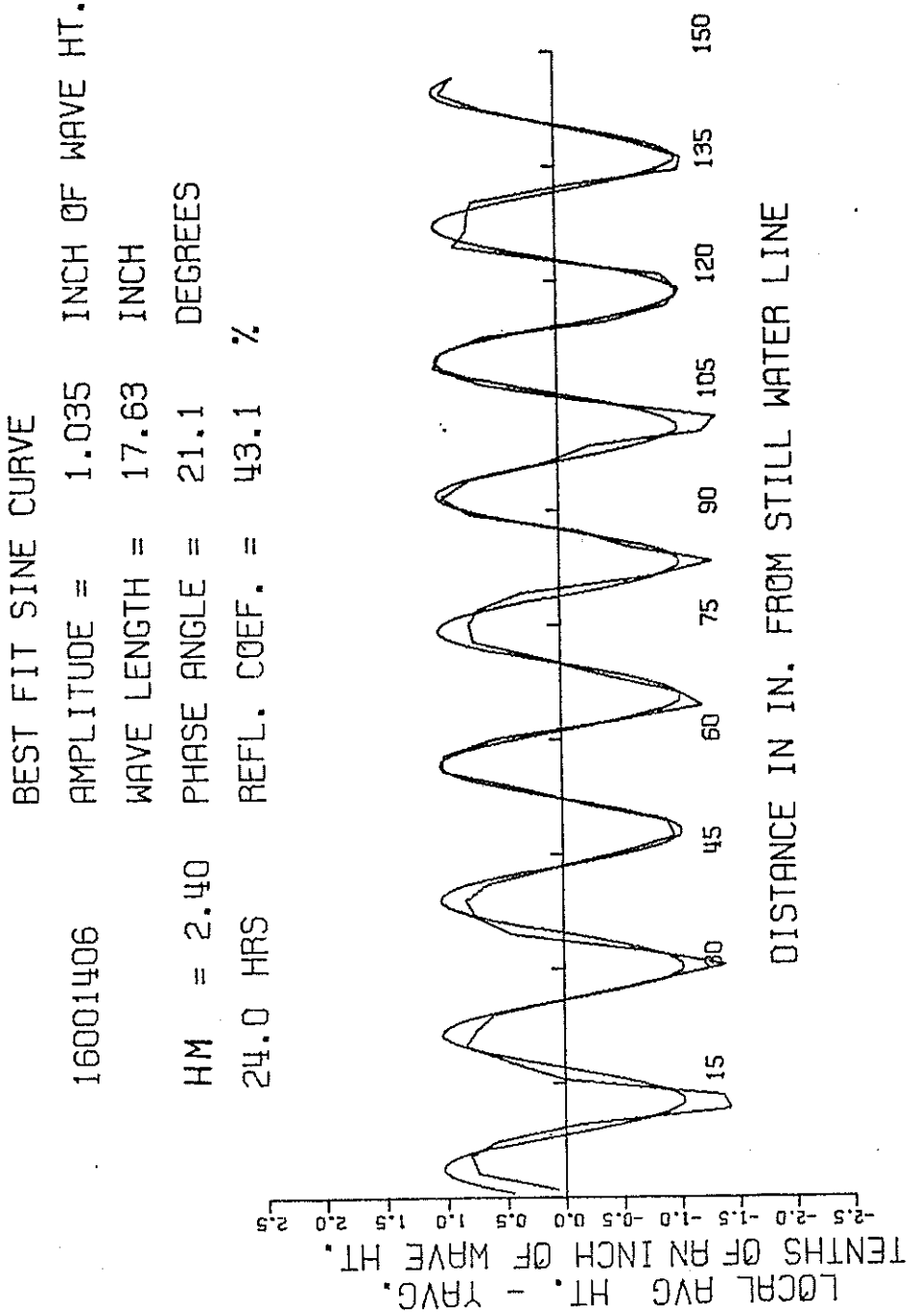

Fig. 5 BEST FIT SINE CURVE FOR CALCULATION OF THE REFLECTION COEFFICIENT

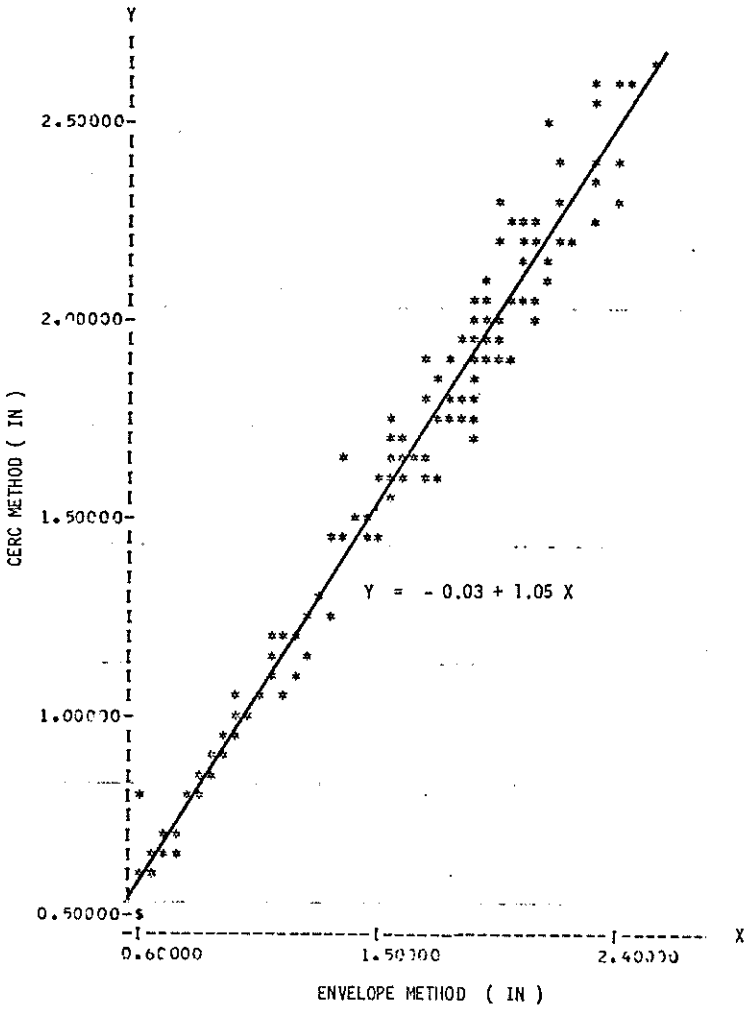

Fig. 6 COMPARISON OF THE CERC METHOD AND THE ENVELOPE METHOD FOR OBTAINING THE INCIDENT WAVE HEIGHT

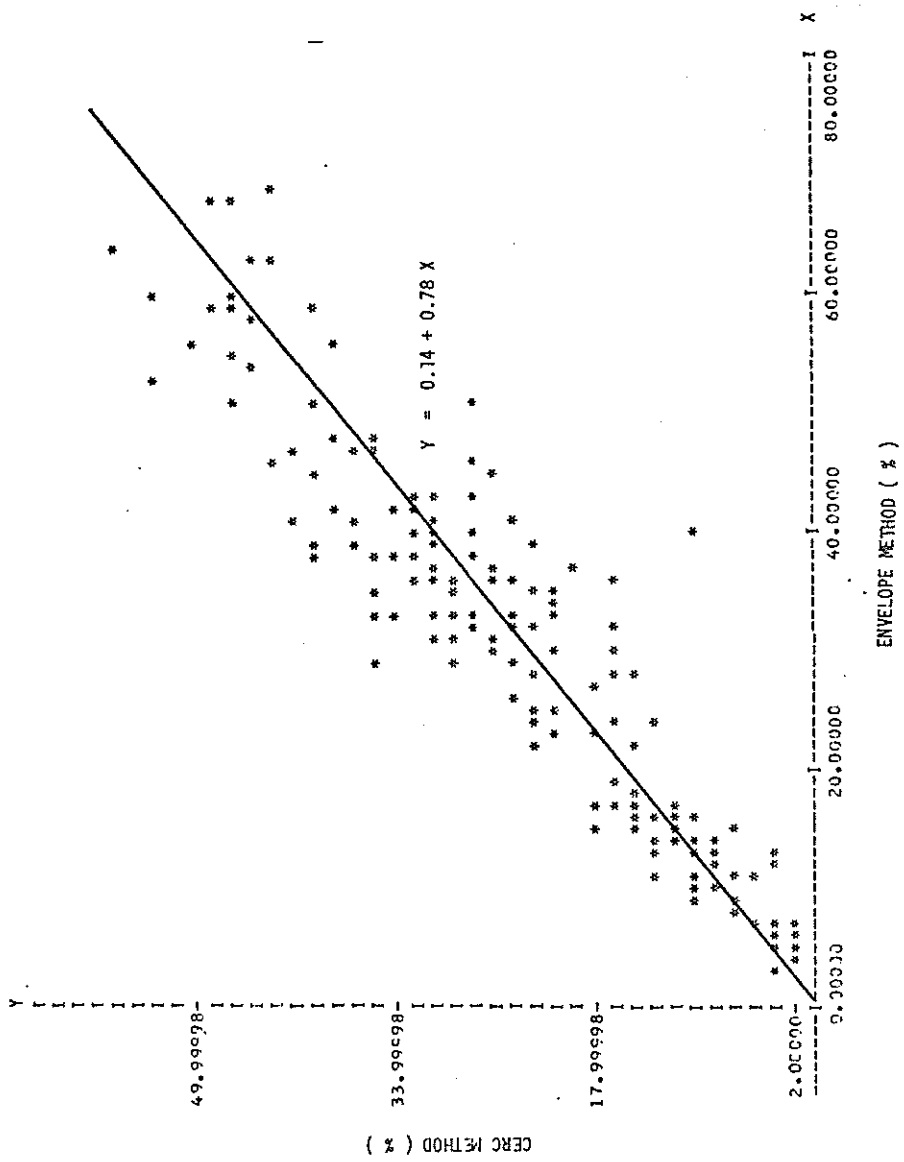

Fig. 7 COMPARISON OF THE CERC METHOD AND THE ENVELOPE METHOD FOR OBTAINING THE REFLECTION COEFFICIENT

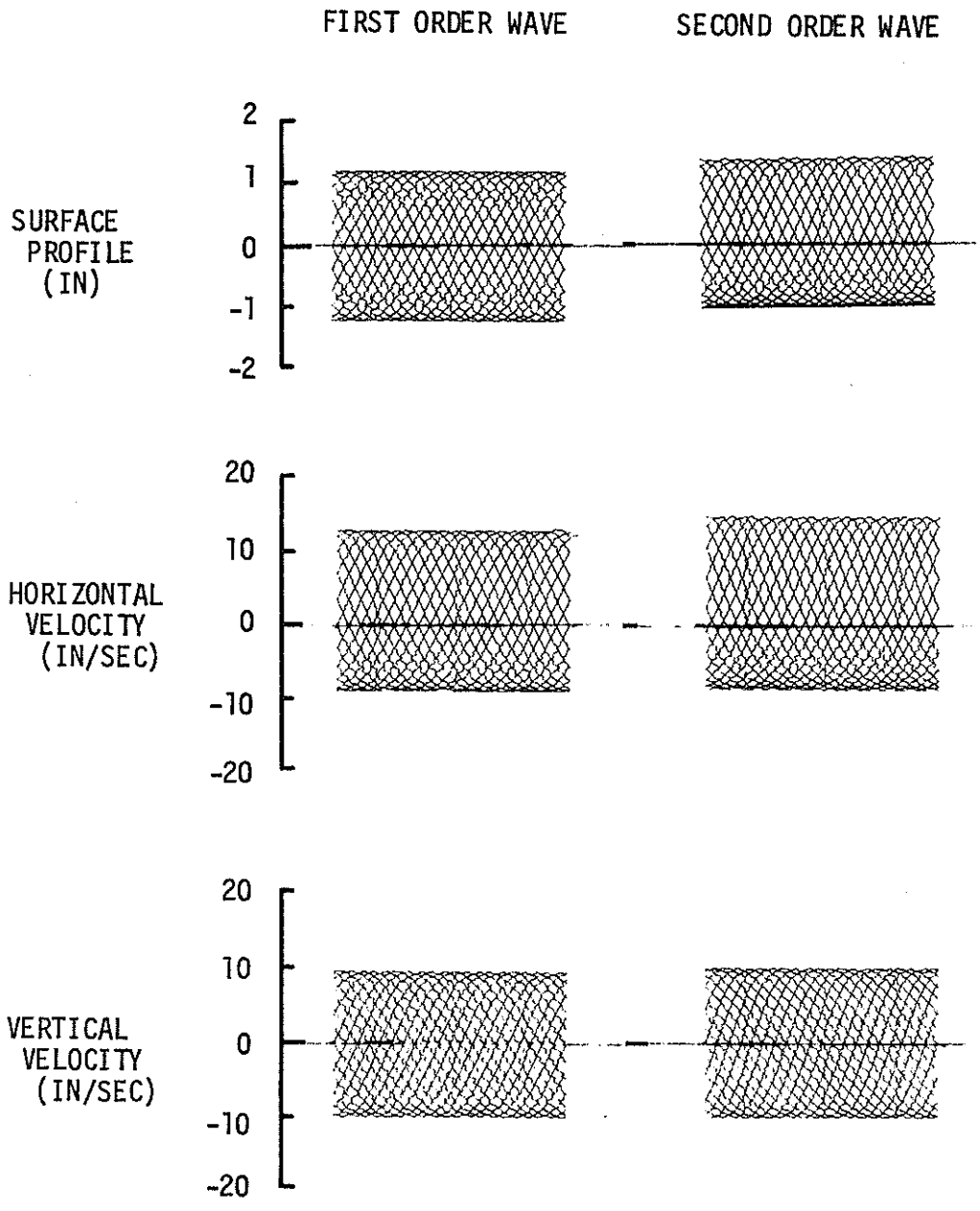

Fig. 8 ENVELOPES FOR A PROGRESSIVE WAVE, R = 0%

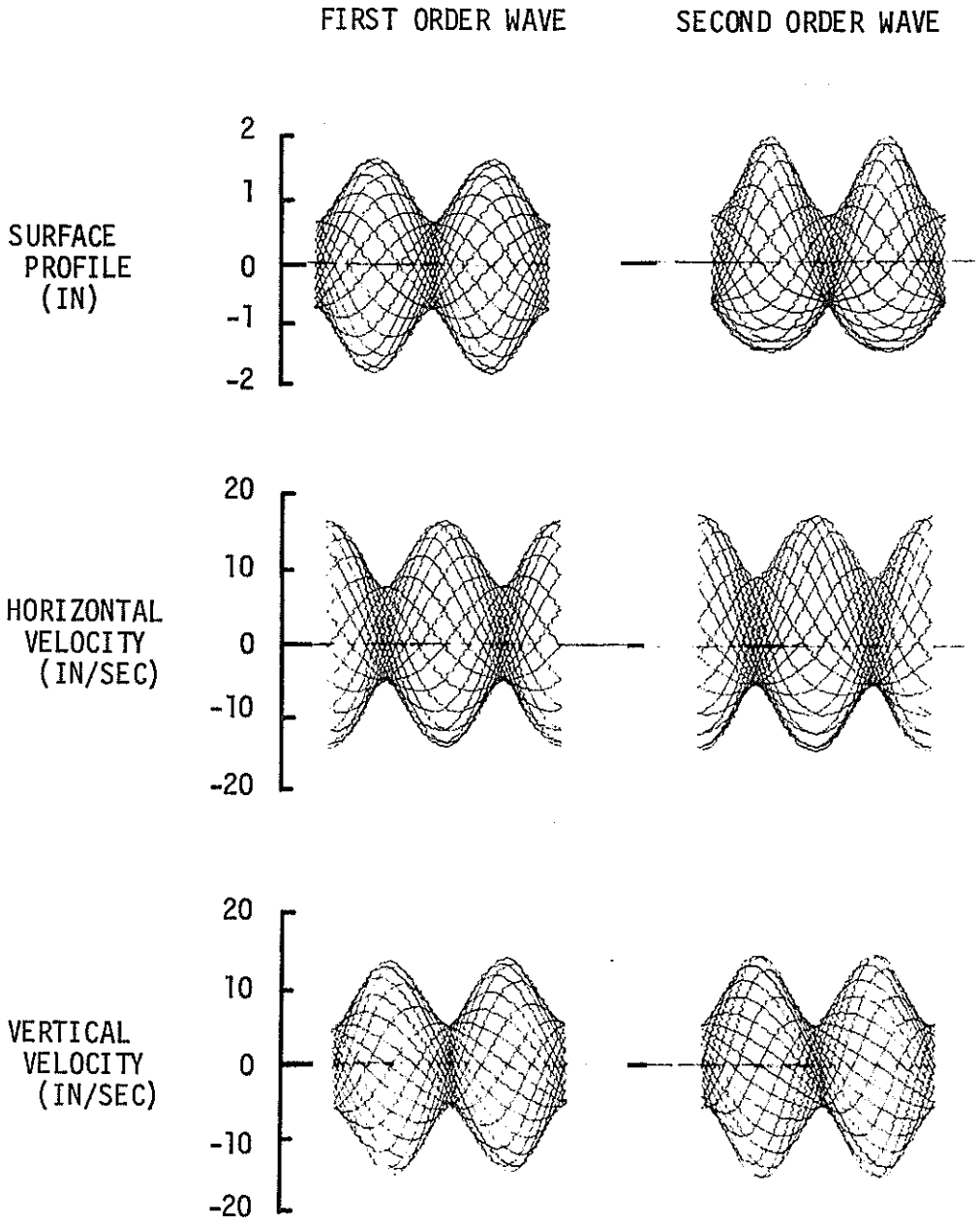

Fig. 9 ENVELOPES FOR A PARTIAL STANDING WAVE, R = 43%

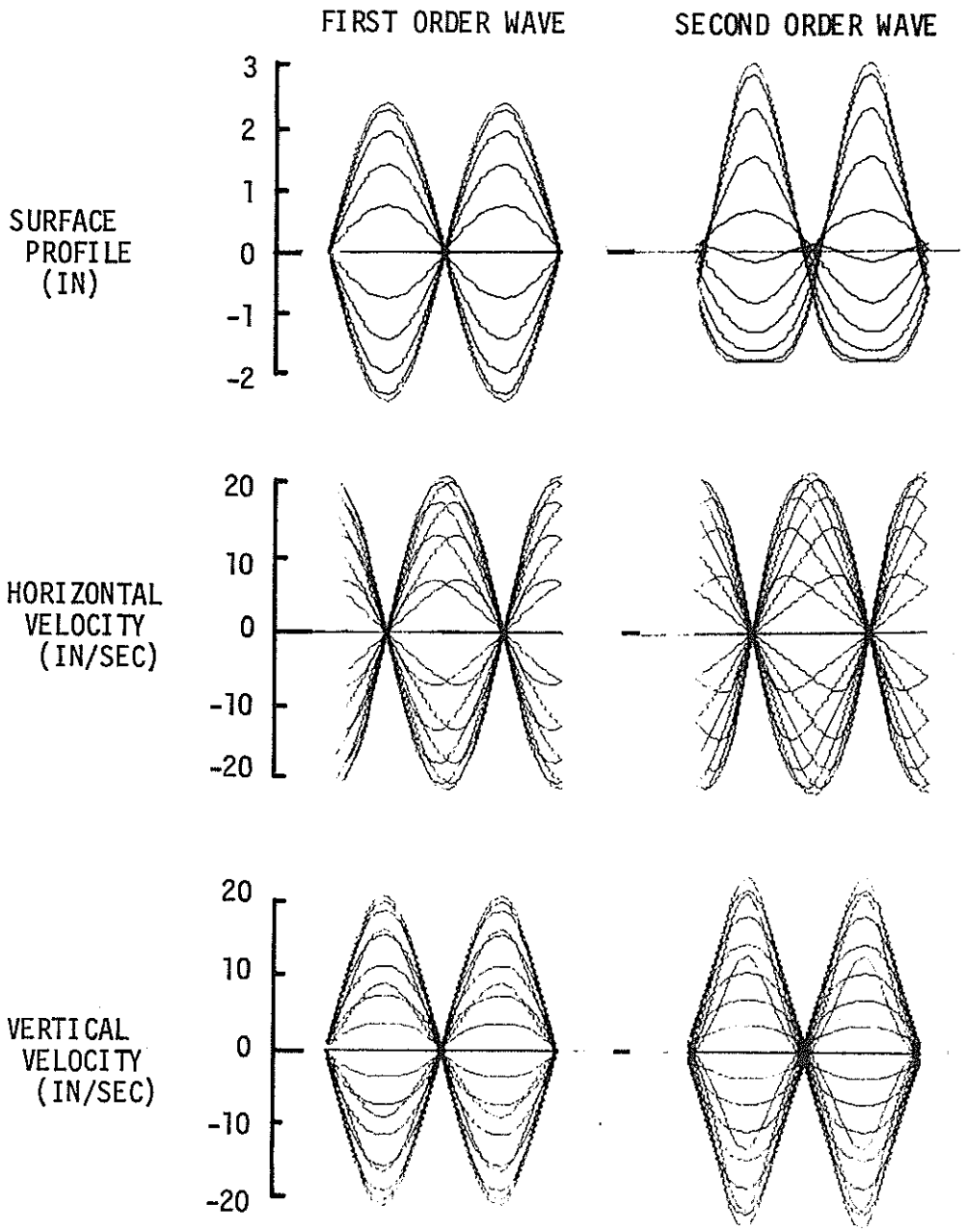

Fig. 10 ENVELOPES FOR A PURE STANDING WAVE, R = 100%

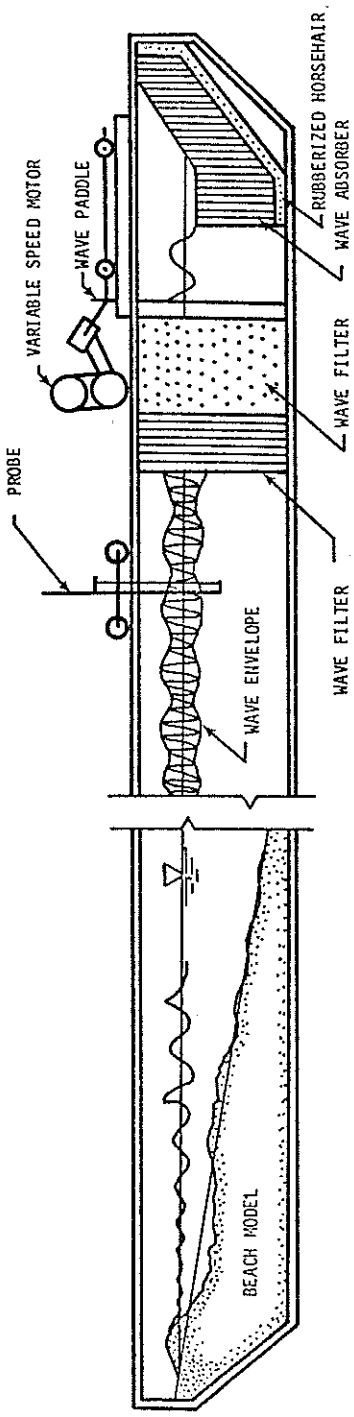

Fig. 11 WAVE TANK

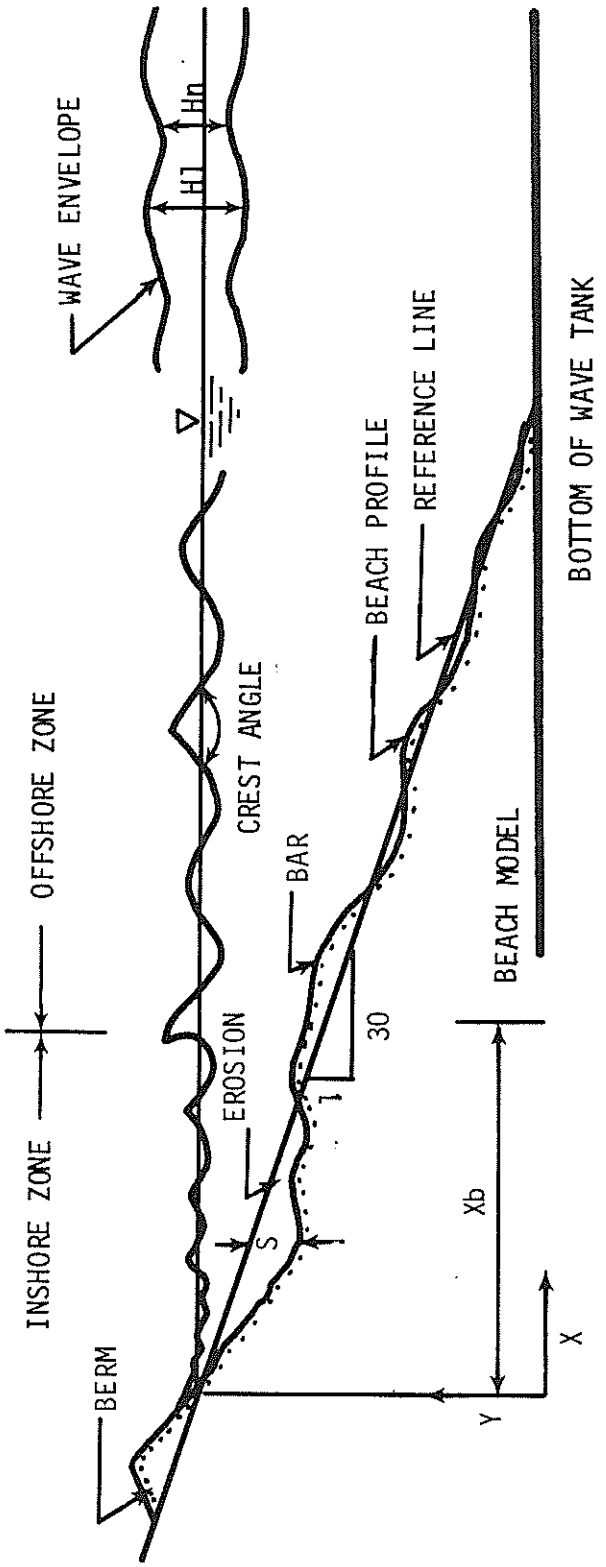

Fig. 12 NOTATION

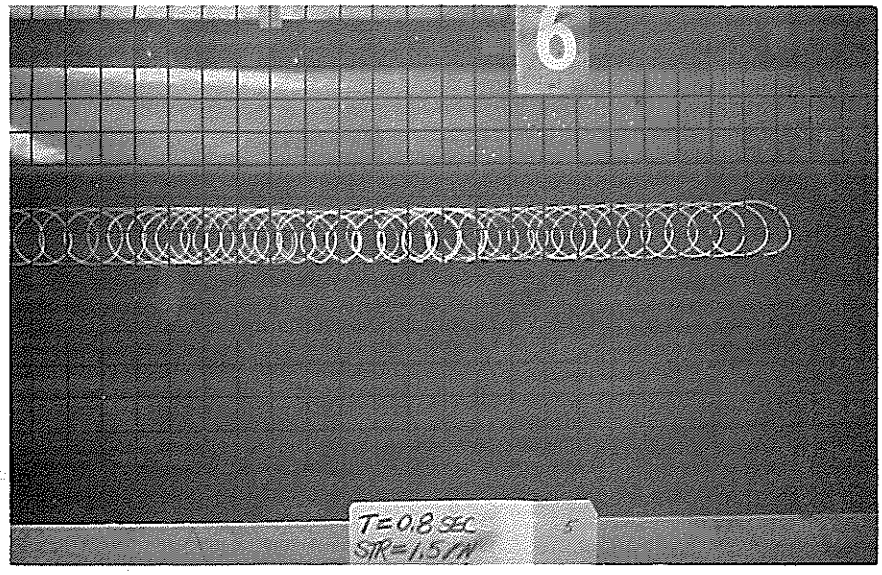

Fig. 13 PARTICLE MOTION FOR THE PROGRESSIVE WAVE CONDITION, STROKE = 1.5 IN.

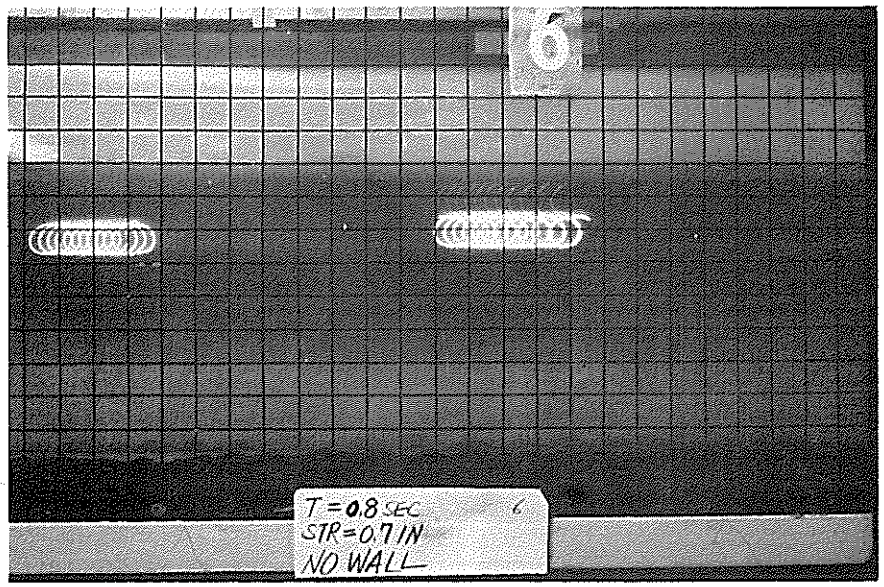

Fig. 14 PARTICLE MOTION FOR THE PROGRESSIVE WAVE CONDITION, STROKE = 0.7 IN.

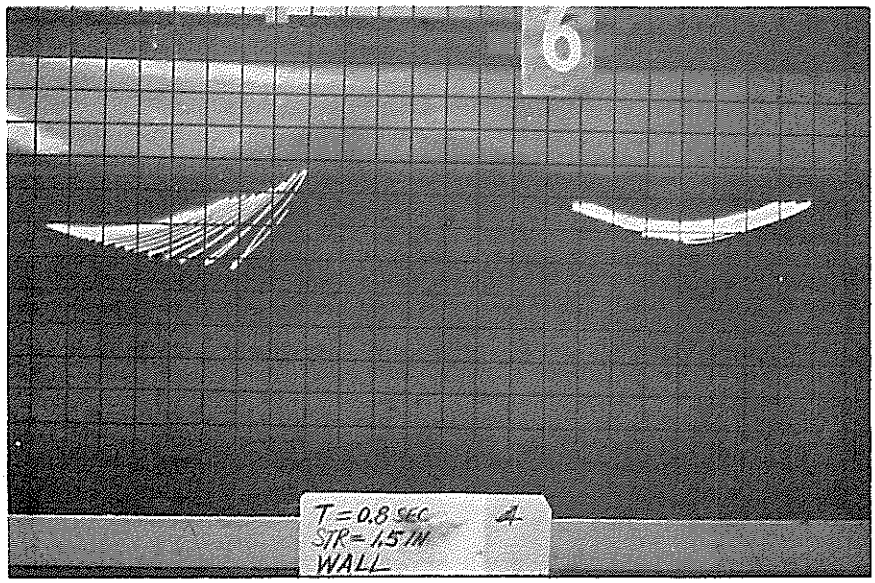

Fig. 15 PARTICLE MOTION FOR THE STANDING WAVE CONDITION, STROKE = 1.5 IN.

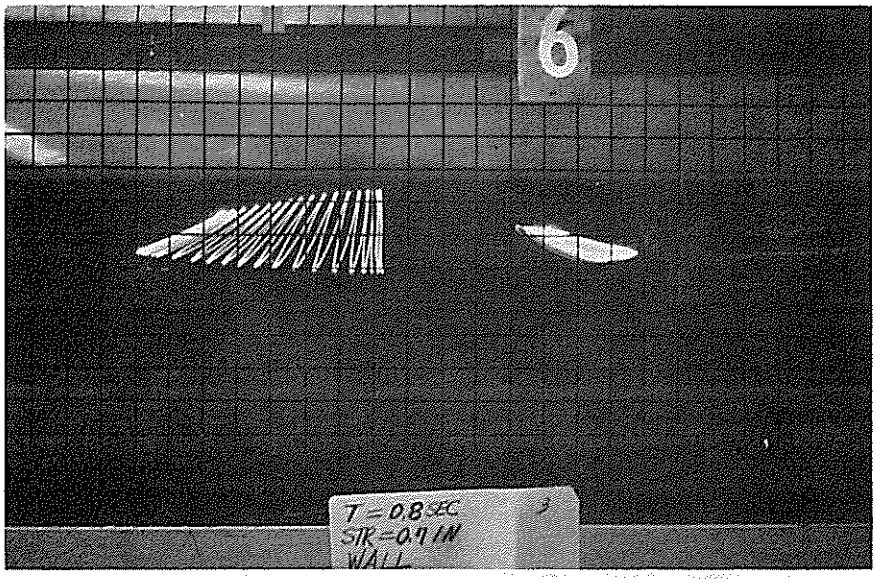

Fig. 16 PARTICLE MOTION FOR THE STANDING WAVE CONDITION, STROKE = 0.7 IN.

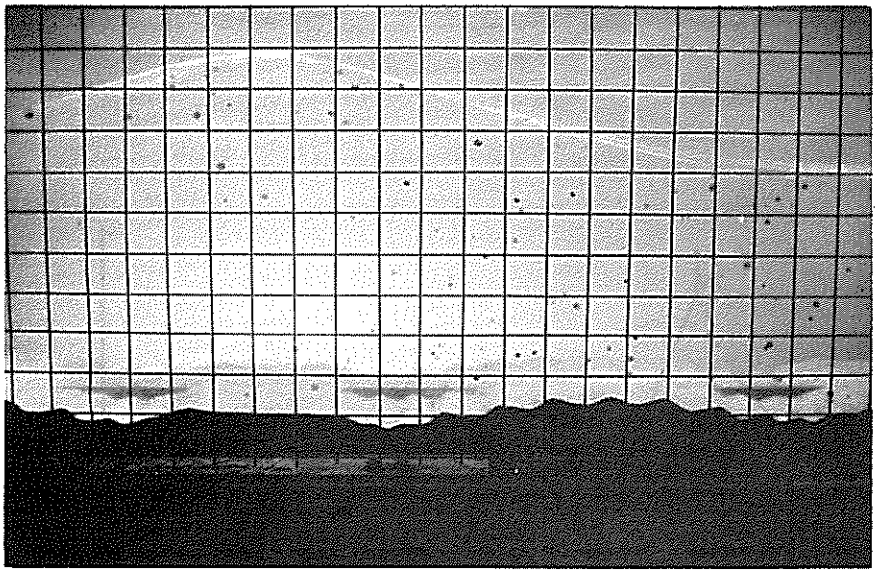

Fig. 17 BEACH DEFORMATION UNDER STANDING WAVE FOR A FLAT BEACH

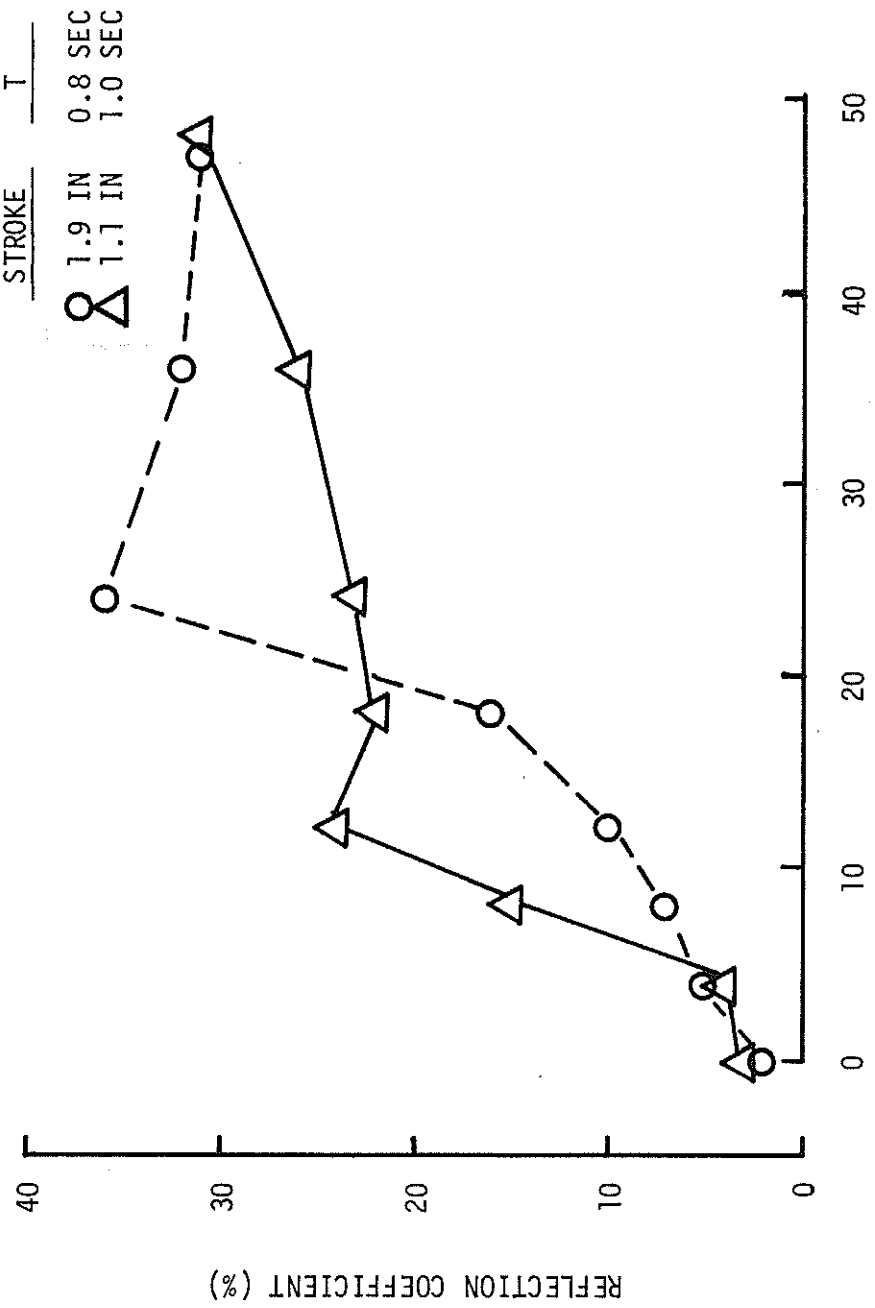

Fig. 18 REFLECTION COEFFICIENT VERSUS DURATION FOR NATURAL BEACHES

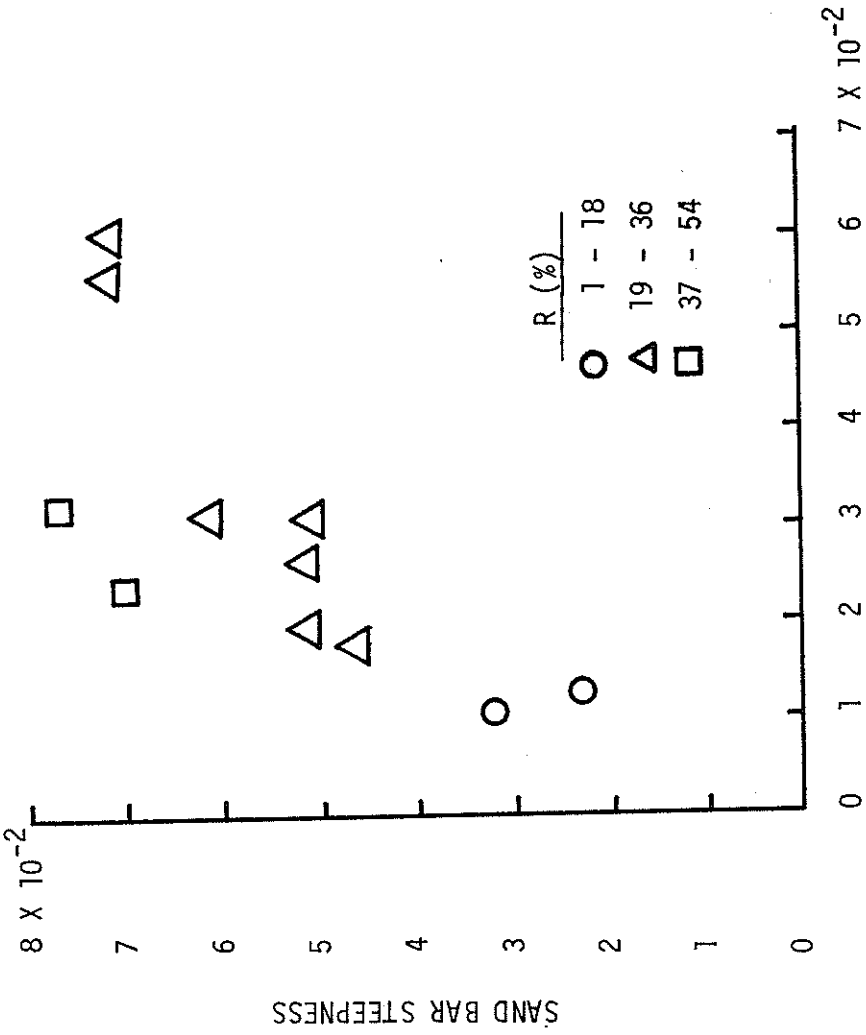

Fig. 19 SAND BAR STEEPNESS VERSUS WAVE STEEPNESS

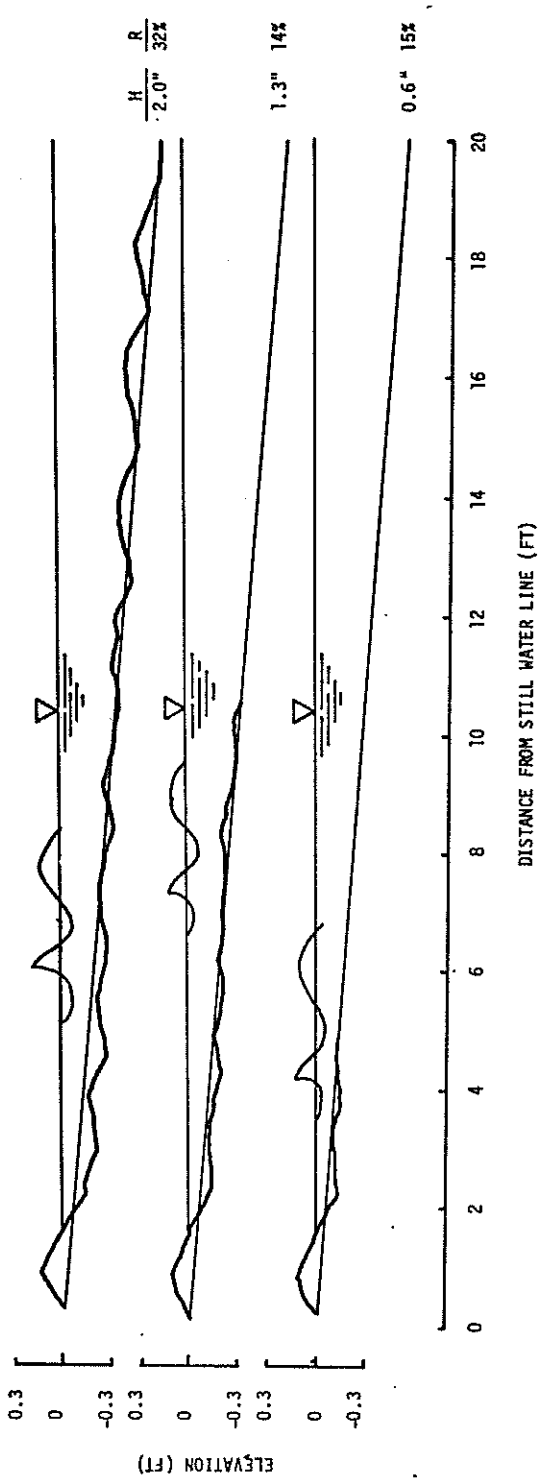

Fig. 20 BEACH PROFILE CHANGE, T = 1.3 SEC.

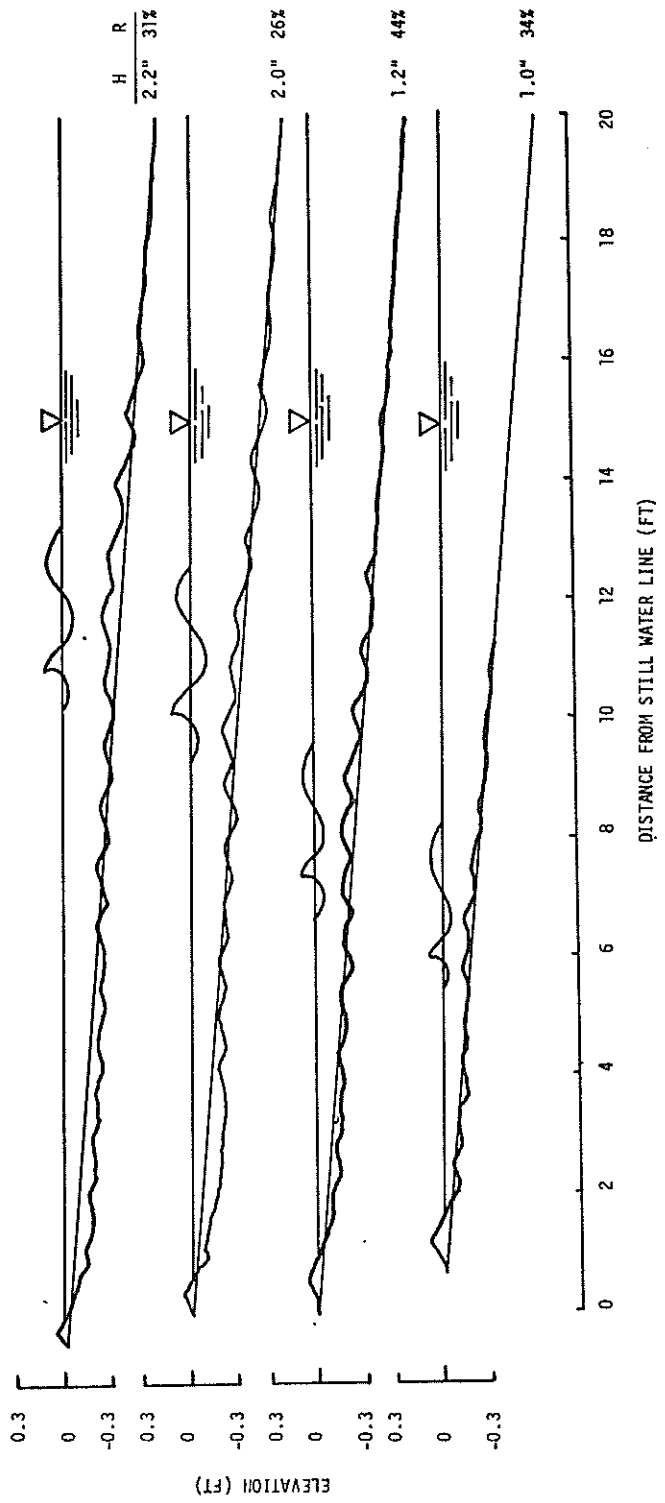

Fig. 21 ·BEACH PROFILE CHANGE, T = 0.8 SEC.

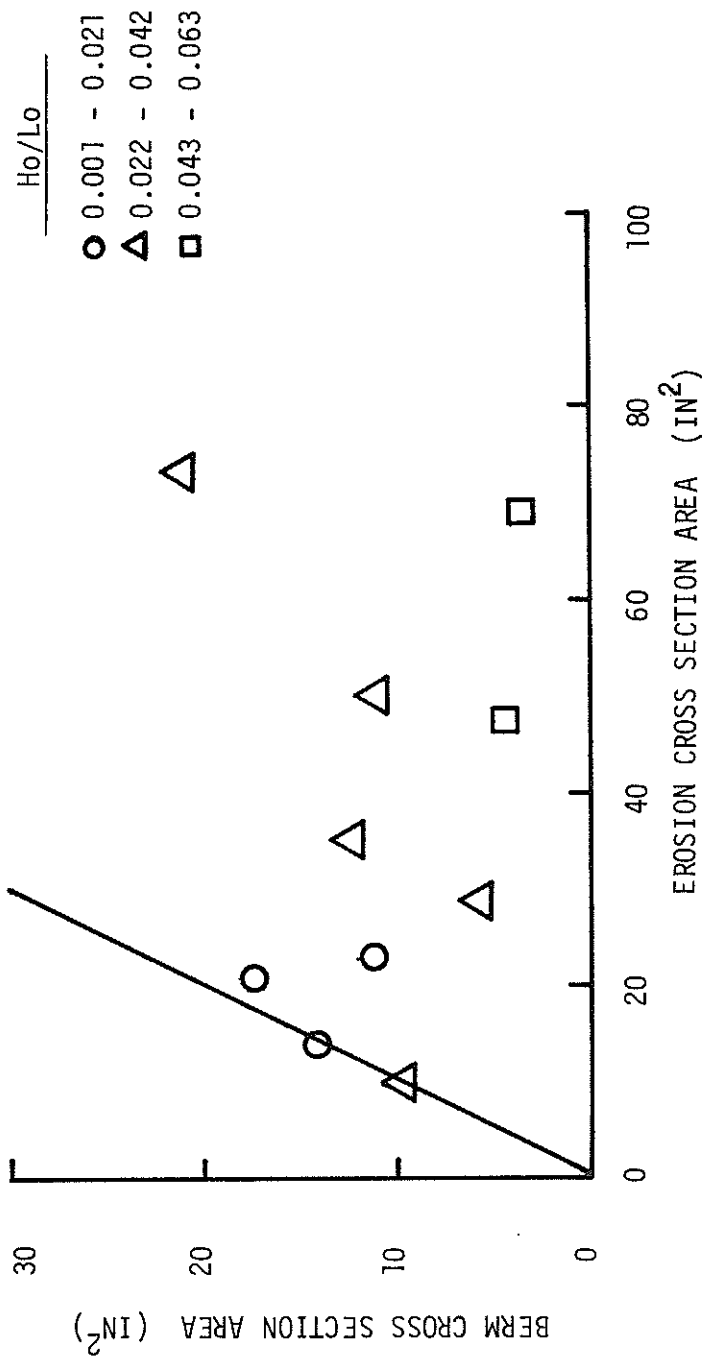

Fig. 22 SAND MOVEMENT IN INSHORE ZONE

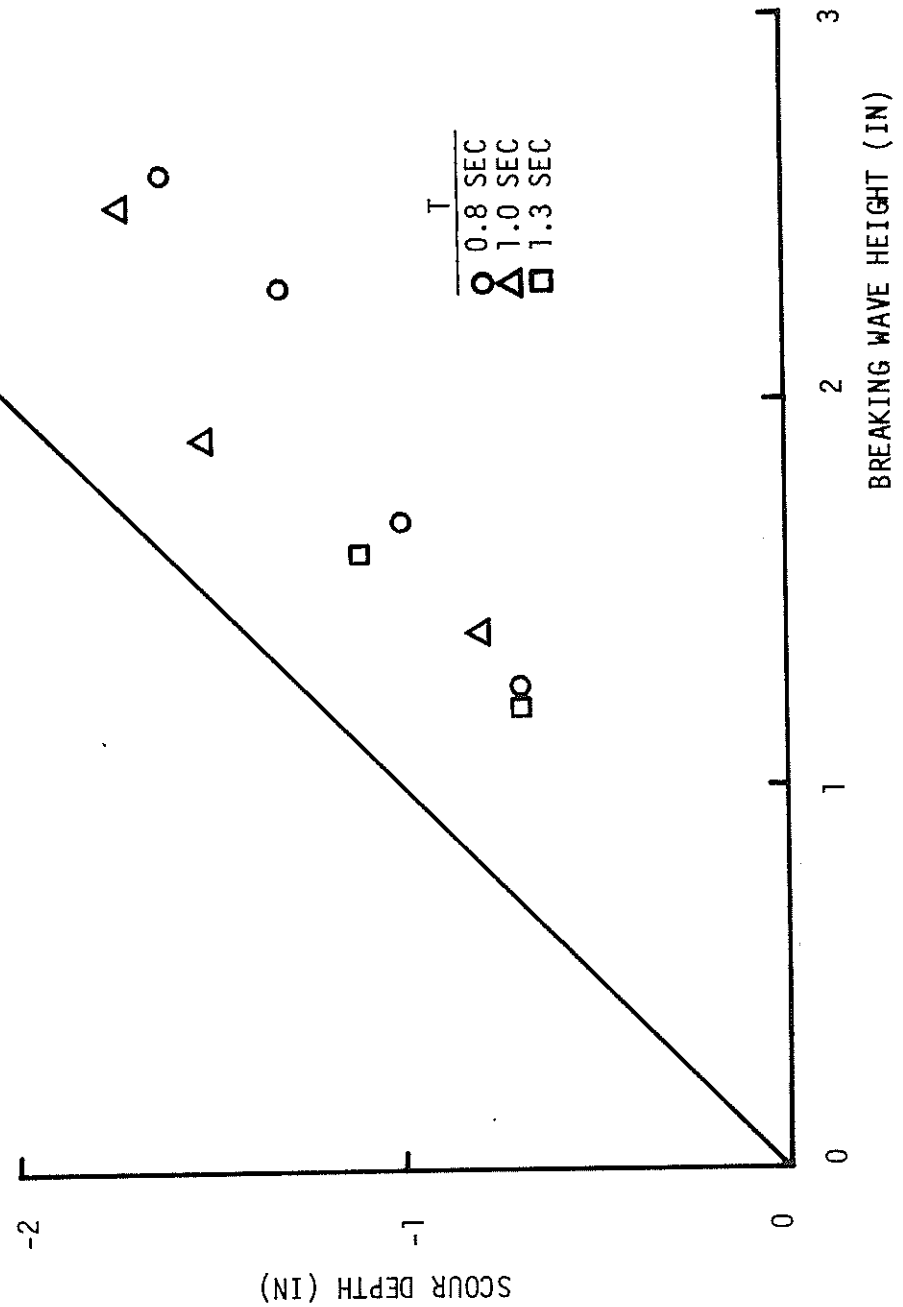

Fig. 23 MAXIMUM ULTIMATE SCOUR DEPTH VERSUS BREAKING WAVE HEIGHT

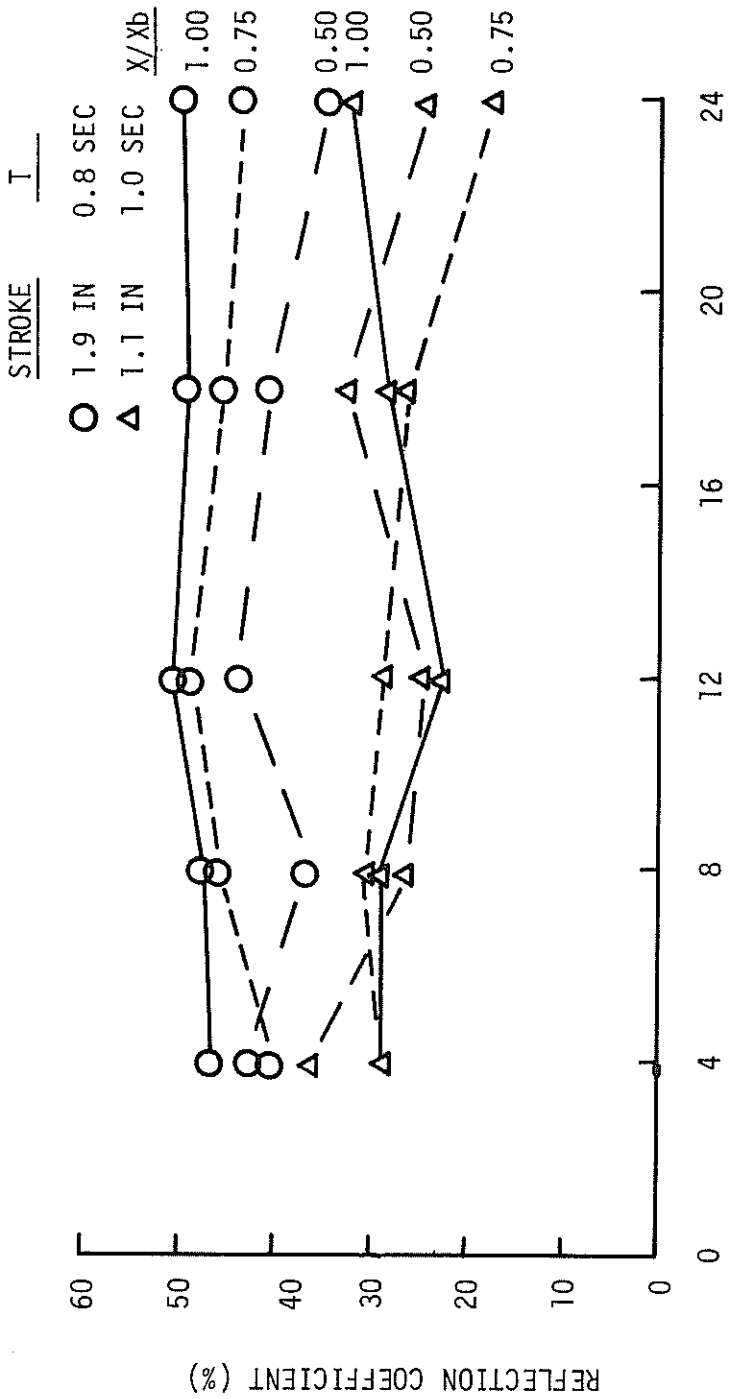

Fig. 24 REFLECTION COEFFICIENT VERSUS DURATION FOR A SEAWALL BEACH

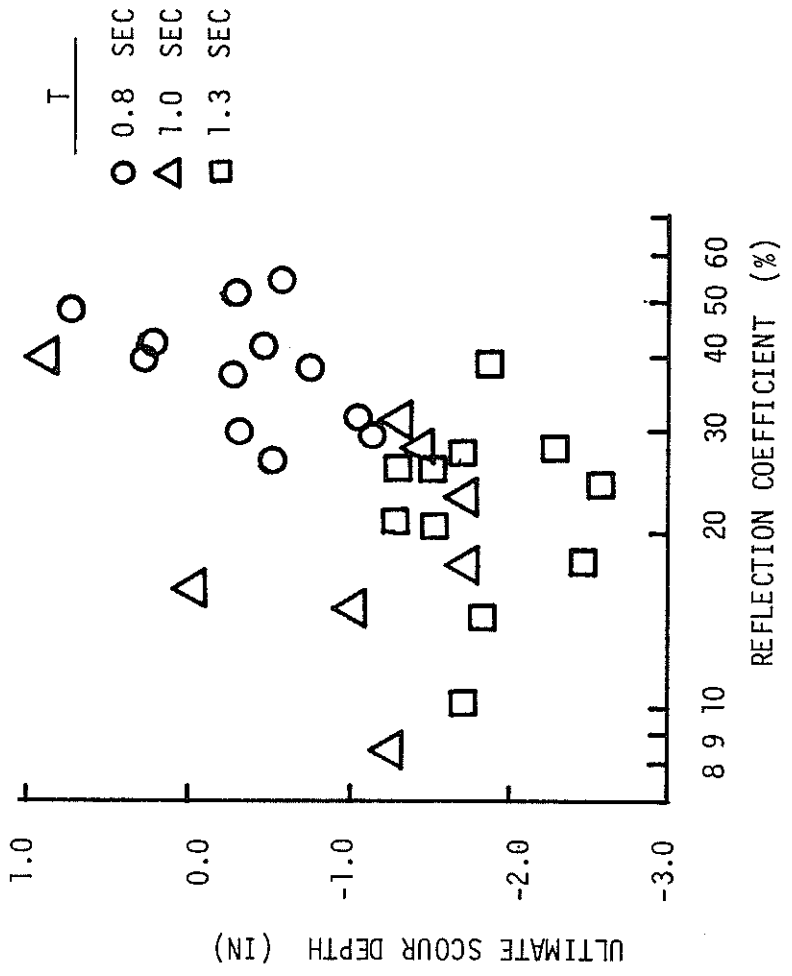

Fig. 25 ULTIMATE SCOUR DEPTH VERSUS REFLECTION COEFFICIENT

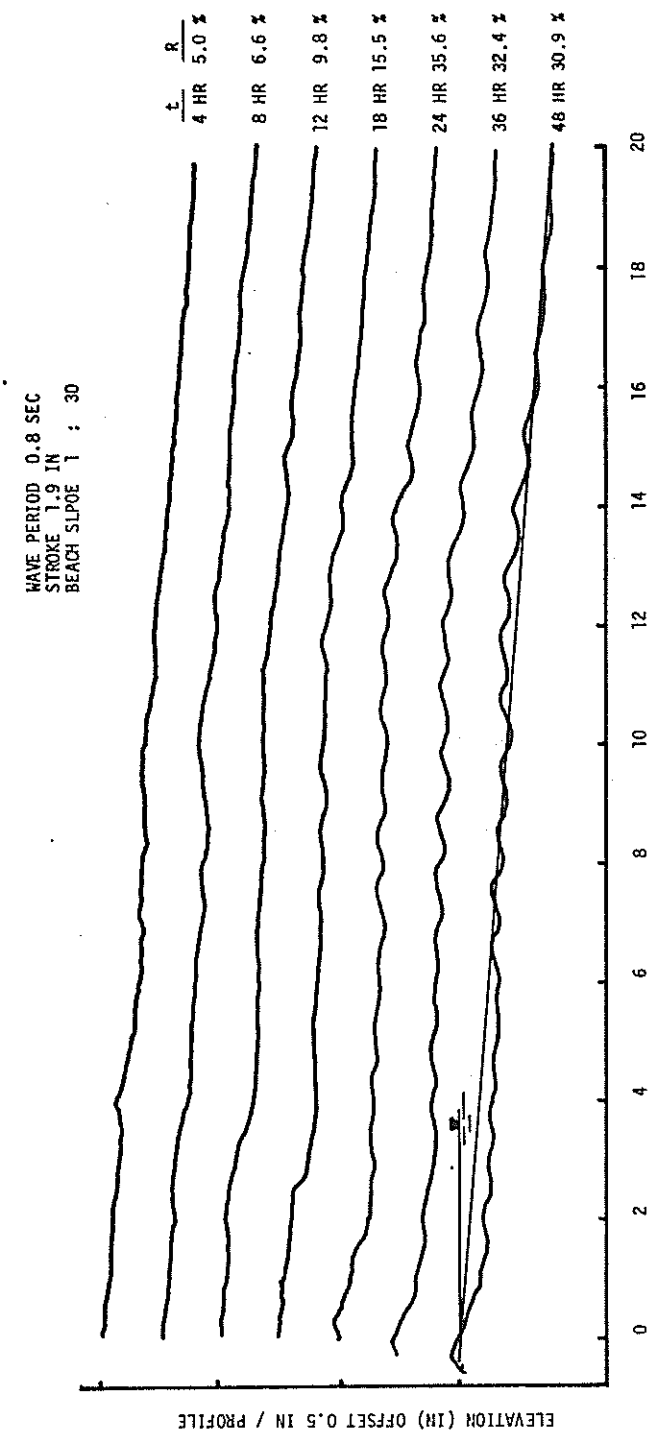

Fig. 26 BEACH PROFILE CHANGE FOR A NATURAL BEACH

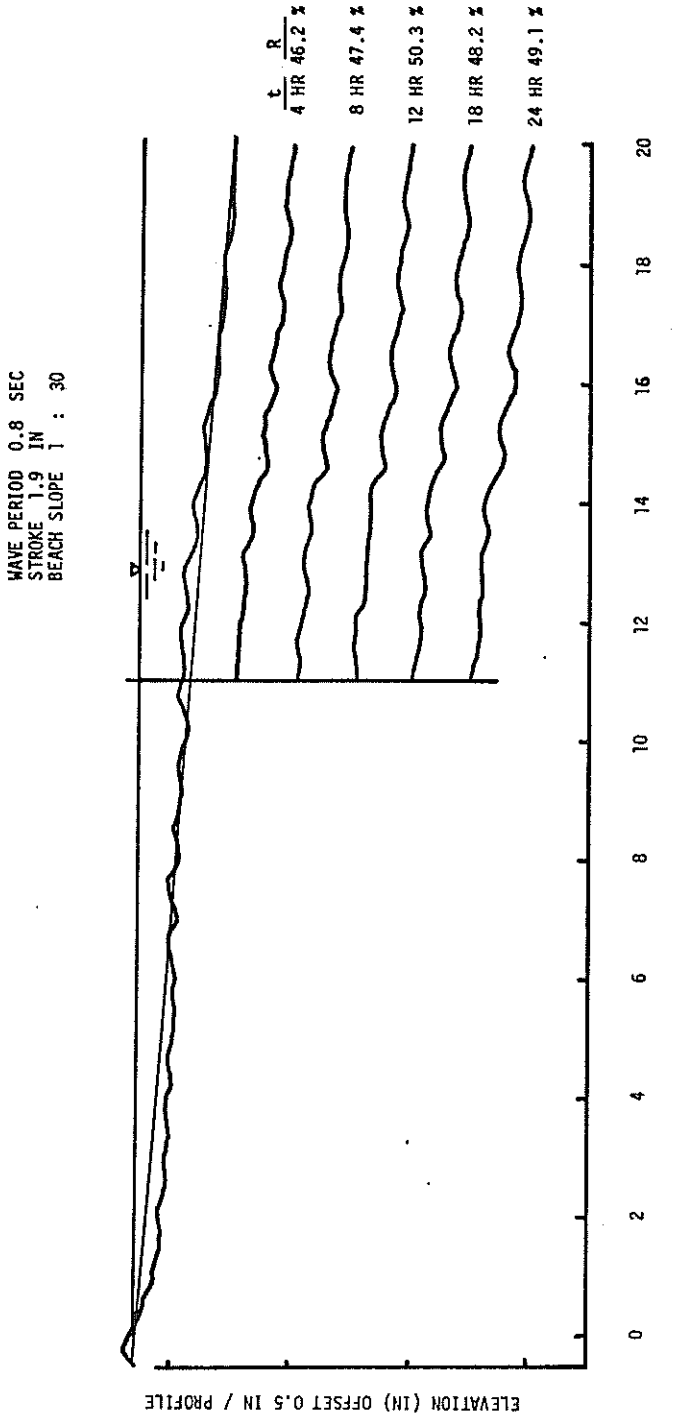

Fig. 27 BEACH PROFILE CHANGE FOR A SEAWALL BEACH, X/Xb = 1.00

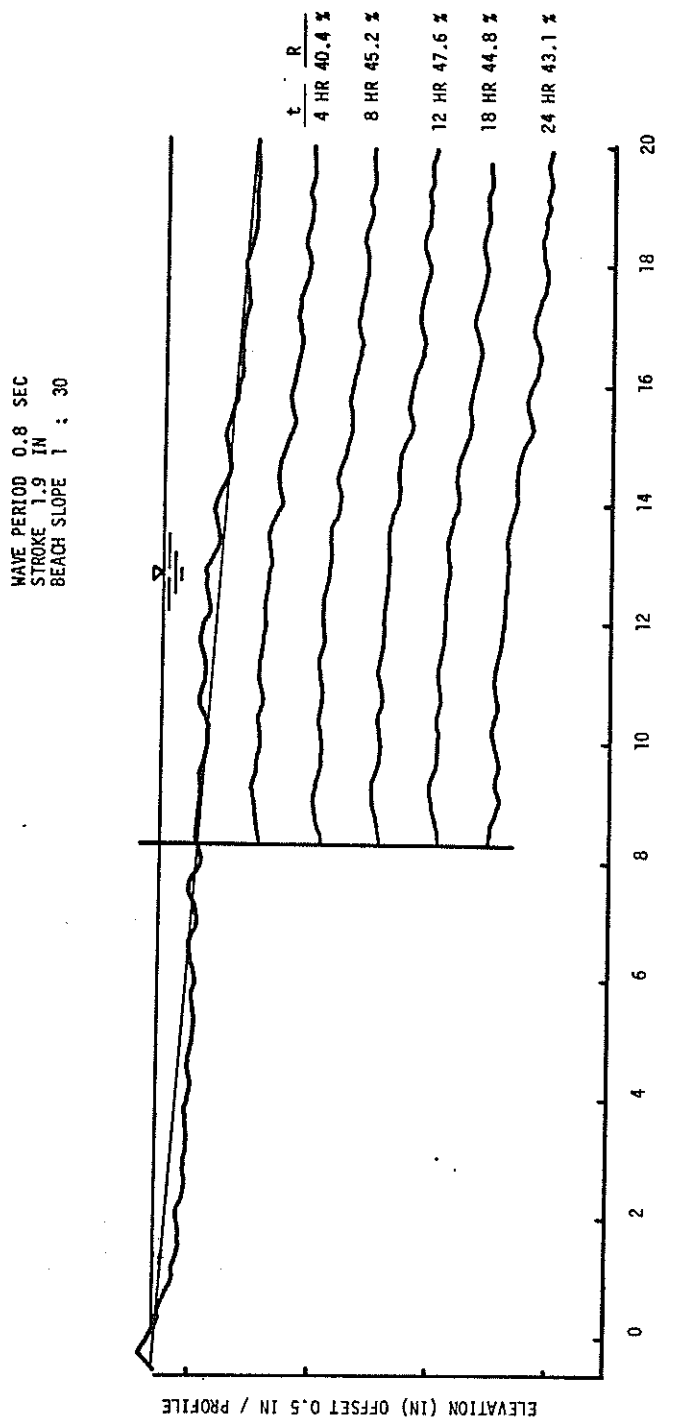

Fig. 28 BEACH PROFILE CHANGE FOR A SEAWALL BEACH, X/Xb = 0.75

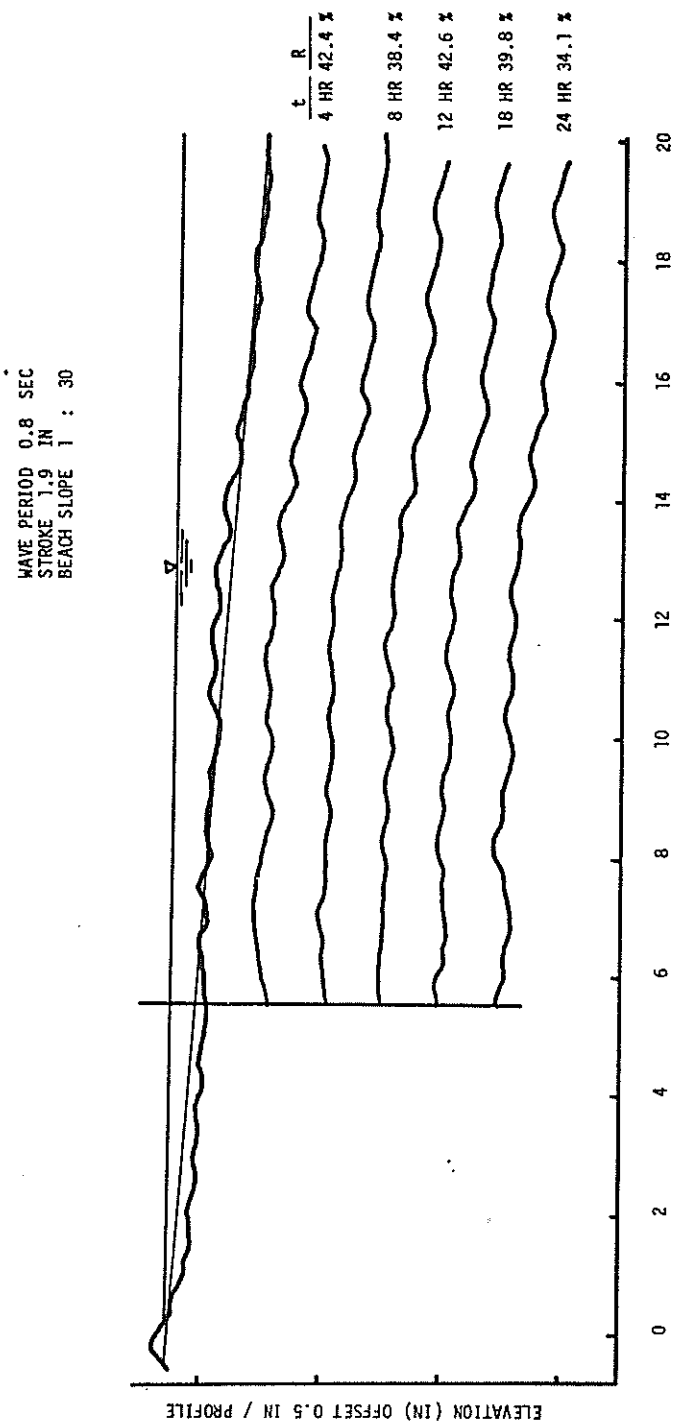

Fig. 29 BEACH PROFILE CHANGE FOR A SEAWALL BEACH, X/Xb = 0.50

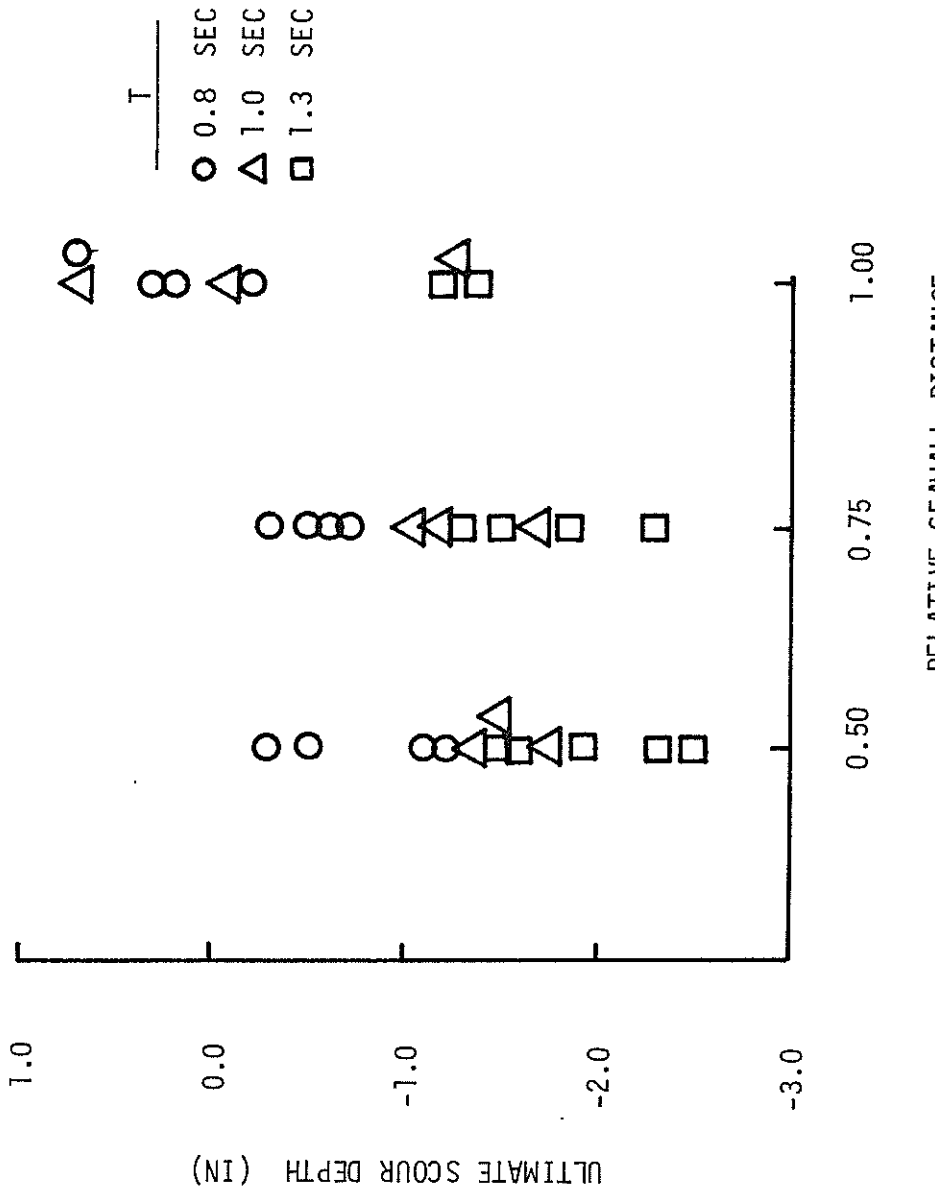

Fig. 30 ULTIMATE SCOUR DEPTH VERSUS RELATIVE SEAWALL DISTANCE

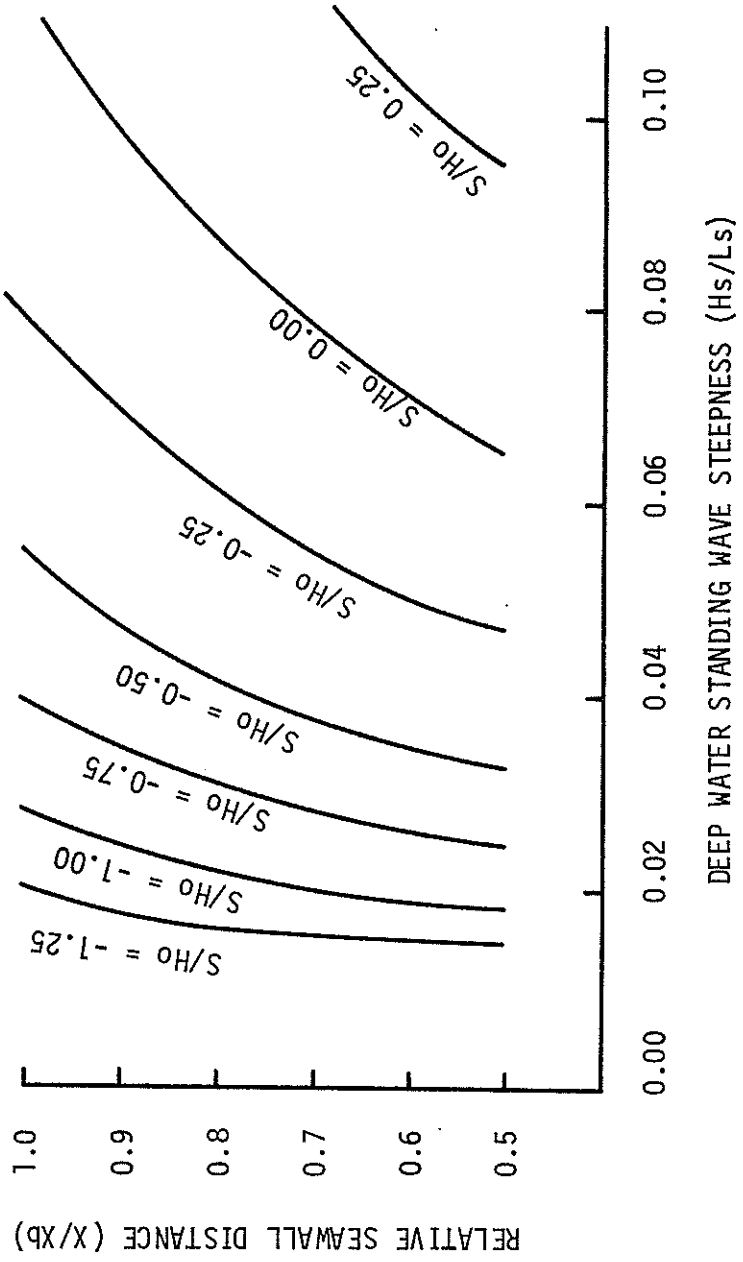

Fig. 31 VARIATION OF RELATIVE SEAWALL DISTANCE WITH DEEP WATER STANDING WAVE STEEPNESS AND RELATIVE SCOUR DEPTH

APPENDIX D

TEST DATA

TABLE 1 NATURAL BEACH TEST

TABLE 2 SEAWALL BEACH TEST

TABLE 1 NATURAL BEACH TEST

T (SEC)	HOUR	LO (IN)	HO (IN)	HB (IN)	R (PER CENT)	HS/LS	HO/LO	S (IN)
1.3	0.	104.	1.5	1.9	3.	0.014	0.014	
1.3	4.	104.	1.6	1.8	4.	0.016	0.015	-0.6
1.3	8.	104.	1.5	1.9	17.	0.017	0.015	-0.9
1.3	12.	104.	1.6	1.9	11.	0.017	0.016	-1.1
1.3	18.	104.	1.7	2.0	13.	0.019	0.017	-1.1
1.3	24.	104.	1.9	2.3	13.	0.020	0.018	-1.3
1.3	36.	104.	2.3	2.2	36.	0.030	0.022	-1.7
1.3	48.	104.	2.5	2.3	38.	0.033	0.024	-2.2
1.3	0.	104.	1.2	1.7	2.	0.011	0.011	
1.3	4.	104.	1.2	1.7	5.	0.012	0.011	-0.3
1.3	10.	104.	1.1	1.6	12.	0.012	0.011	-0.5
1.3	12.	104.	1.1	1.6	11.	0.012	0.011	-0.5
1.3	18.	104.	1.1	1.6	8.	0.012	0.011	-0.8
1.3	24.	104.	1.0	1.7	16.	0.012	0.010	-1.0
1.3	36.	104.	1.1	1.6	13.	0.012	0.010	-1.0
1.3	48.	104.	1.1	1.6	12.	0.012	0.011	-1.1
1.3	0.	104.	0.7	1.2	4.	0.007	0.007	
1.3	4.	104.	0.7	1.2	12.	0.007	0.007	-0.3
1.3	8.	104.	0.6	1.2	8.	0.006	0.006	-0.6
1.3	12.	104.	0.7	1.2	4.	0.007	0.007	-0.5
1.3	18.	104.	0.6	1.2	17.	0.007	0.006	-0.7
1.3	24.	104.	0.7	1.2	9.	0.007	0.006	-0.7
1.3	36.	104.	0.6	1.2	13.	0.007	0.006	-0.7
1.3	48.	104.	0.7	1.2	9.	0.007	0.007	-0.7

TABLE 2 SEAWALL BEACH TEST

T (SEC)	HOUR	LO (IN)	HO (IN)	R (PER CENT)	HS/LS	HO/LO	S (IN)	RX
1.3	4.	104.	2.0	24.	0.023	0.019	-2.3	0.50
1.3	8.	104.	2.1	23.	0.025	0.020	-2.4	0.50
1.3	12.	104.	1.8	25.	0.022	0.017	-2.6	0.50
1.3	18.	104.	1.9	25.	0.023	0.018	-2.6	0.50
1.3	24.	104.	2.0	25.	0.024	0.019	-2.6	0.50
1.3	24.	104.	1.9	28.	0.023	0.018	-1.7	1.00
1.3	24.	104.	1.7	28.	0.021	0.016	-2.3	0.75
1.3	24.	104.	1.9	18.	0.022	0.018	-2.4	0.51
1.3	4.	104.	1.2	32.	0.015	0.011	-1.5	0.49
1.3	8.	104.	1.3	30.	0.016	0.012	-1.7	0.49
1.3	12.	104.	1.2	29.	0.015	0.012	-1.1	0.49
1.3	18.	104.	1.3	36.	0.016	0.012	-1.7	0.49
1.3	24.	104.	1.3	26.	0.015	0.012	-1.6	0.49
1.3	24.	104.	1.6	25.	0.020	0.016	-1.3	1.00
1.3	24.	104.	1.6	21.	0.018	0.015	-1.3	0.75
1.3	24.	104.	1.7	39.	0.022	0.016	-1.9	0.50
1.3	4.	104.	0.8	21.	0.010	0.008	-1.2	0.60
1.3	8.	104.	0.7	22.	0.008	0.007	-1.3	0.60
1.3	12.	104.	0.8	16.	0.008	0.007	-1.3	0.60
1.3	18.	104.	0.7	25.	0.008	0.006	-1.4	0.60
1.3	24.	104.	0.7	21.	0.009	0.007	-1.5	0.60
1.3	24.	104.	0.9	15.	0.010	0.009	-1.8	0.76
1.3	24.	104.	0.8	10.	0.009	0.008	-1.7	0.50
1.0	4.	61.	2.0	43.	0.046	0.032	0.6	1.00

TABLE 2 SEAWALL BEACH TEST (CONTINUED)

T (SEC)	HOUR	LO (IN)	HO (IN)	R (PER CENT)	HS/LS	HO/LO	S (IN)	RX
1.0	8.	61.	1.9	47.	0.045	0.031	0.7	1.00
1.0	12.	61.	2.1	30.	0.044	0.034	1.0	1.00
1.0	18.	61.	2.1	26.	0.043	0.034	0.9	1.00
1.0	24.	61.	1.9	41.	0.043	0.031	0.9	1.00
1.0	4.	61.	2.1	31.	0.045	0.035	-0.9	0.75
1.0	8.	61.	2.1	30.	0.045	0.034	-0.9	0.75
1.0	12.	61.	2.3	29.	0.047	0.037	-1.0	0.75
1.0	18.	61.	1.8	48.	0.042	0.029	-1.1	0.75
1.0	24.	61.	2.0	31.	0.042	0.032	-1.2	0.75
1.0	4.	61.	1.9	33.	0.042	0.032	-0.8	0.50
1.0	8.	61.	2.1	38.	0.048	0.035	-0.9	0.50
1.0	12.	61.	2.3	31.	0.048	0.037	-1.0	0.50
1.0	18.	61.	2.2	36.	0.048	0.035	-1.1	0.50
1.0	24.	61.	2.3	28.	0.047	0.037	-1.5	0.50
1.0	4.	61.	2.0	28.	0.041	0.032	-0.3	1.00
1.0	8.	61.	1.9	29.	0.040	0.031	-1.0	1.00
1.0	12.	61.	1.9	22.	0.037	0.030	-1.1	1.00
1.0	18.	61.	1.9	28.	0.039	0.030	-1.2	1.00
1.0	24.	61.	1.8	32.	0.038	0.029	-1.3	1.00
1.0	4.	61.	1.8	28.	0.037	0.029	-1.4	0.75
1.0	8.	61.	1.8	30.	0.038	0.029	-1.4	0.75
1.0	12.	61.	1.7	28.	0.034	0.027	-1.7	0.75
1.0	18.	61.	1.8	26.	0.036	0.029	-1.7	0.75
1.0	24.	61.	1.8	17.	0.035	0.029	-1.8	0.75

TABLE 2 SEAWALL BEACH TEST (CONTINUED)

T (SEC)	HOUR	LO (IN)	HO (IN)	R (PER CENT)	HS/LS	HO/LO	S (IN)	RX
1.0	4.	61.	1.8	36.	0.039	0.029	-1.6	0.51
1.0	8.	61.	1.8	26.	0.037	0.029	-1.7	0.51
1.0	12.	61.	1.8	24.	0.036	0.029	-1.7	0.51
1.0	16.	61.	1.6	32.	0.035	0.026	-1.7	0.51
1.0	24.	61.	1.8	24.	0.036	0.029	-1.7	0.51
1.0	4.	61.	1.3	16.	0.025	0.021	-0.2	1.00
1.0	8.	61.	1.3	18.	0.025	0.021	-0.2	1.00
1.0	12.	61.	1.3	17.	0.025	0.021	-0.1	1.00
1.0	18.	61.	1.3	17.	0.025	0.021	-0.1	1.00
1.0	24.	61.	1.3	16.	0.025	0.021	-0.1	1.00
1.0	4.	61.	1.4	29.	0.029	0.022	-1.1	0.75
1.0	8.	61.	1.6	20.	0.031	0.026	-1.0	0.75
1.0	12.	61.	1.6	17.	0.031	0.027	-1.0	0.75
1.0	18.	61.	1.6	20.	0.031	0.026	-1.0	0.75
1.0	24.	61.	1.6	15.	0.029	0.025	-1.1	0.75
1.0	4.	61.	1.0	11.	0.018	0.016	-1.2	0.51
1.0	8.	61.	0.9	16.	0.018	0.015	-1.4	0.51
1.0	12.	61.	1.0	15.	0.019	0.017	-1.1	0.51
1.0	18.	61.	1.1	14.	0.019	0.017	-1.3	0.51
1.0	24.	61.	1.0	9.	0.018	0.017	-1.3	0.51
0.8	4.	39.	2.2	56.	0.086	0.055	0.2	1.00
0.8	8.	39.	2.3	47.	0.085	0.058	0.4	1.00
0.8	12.	39.	2.3	45.	0.085	0.058	0.2	1.00
0.8	18.	39.	2.4	41.	0.087	0.062	0.2	1.00

TABLE 2 SEAWALL BEACH TEST (CONTINUED)

T (SEC)	HOUR	LO (IN)	HO (IN)	R (PER CENT)	HS/LS	HO/LO	S (IN)	RX
0.8	24.	39.	2.4	44.	0.087	0.061	0.2	1.00
0.8	4.	39.	2.1	34.	0.071	0.053	-0.6	0.75
0.8	8.	39.	2.0	30.	0.066	0.050	-0.6	0.75
0.8	12.	39.	2.0	29.	0.065	0.050	-0.6	0.75
0.8	18.	39.	2.0	30.	0.066	0.051	-0.5	0.75
0.8	24.	39.	1.8	39.	0.064	0.046	-0.8	0.75
0.8	4.	39.	2.2	36.	0.077	0.057	-0.5	0.49
0.8	8.	39.	2.1	30.	0.070	0.054	-1.1	0.49
0.8	12.	39.	2.3	34.	0.078	0.058	-1.0	0.49
0.8	18.	39.	2.3	32.	0.076	0.058	-1.2	0.49
0.8	24.	39.	2.1	30.	0.069	0.053	-1.2	0.49
0.8	4.	39.	2.9	46.	0.106	0.073	0.9	1.00
0.8	8.	39.	2.8	47.	0.106	0.072	0.8	1.00
0.8	12.	39.	2.8	50.	0.109	0.072	0.9	1.00
0.8	18.	39.	2.5	48.	0.093	0.063	0.7	1.00
0.8	24.	39.	2.5	49.	0.094	0.063	0.7	1.00
0.8	4.	39.	2.9	40.	0.102	0.073	-0.2	0.75
0.8	8.	39.	2.8	45.	0.102	0.071	-0.2	0.75
0.8	12.	39.	2.8	48.	0.105	0.071	-0.3	0.75
0.8	18.	39.	2.7	45.	0.100	0.069	-0.3	0.75
0.8	24.	39.	2.6	43.	0.095	0.066	-0.5	0.75
0.8	4.	39.	2.6	42.	0.095	0.067	-1.2	0.50
0.8	8.	39.	2.8	38.	0.097	0.070	-1.1	0.50
0.8	12.	39.	2.4	43.	0.089	0.062	-0.7	0.50

TABLE 2 SEAWALL BEACH TEST (CONTINUED)

T (SEC)	HOUR	LO (IN)	HO (IN)	R (PER CENT)	HS/LS	HO/LO	S (IN)	RX
0.8	18.	39.	2.6	40.	0.094	0.067	-0.7	0.50
0.8	24.	39.	2.6	34.	0.089	0.066	-1.1	0.50
0.8	24.	39.	1.3	53.	0.051	0.033	-0.3	1.00
0.8	24.	39.	1.3	37.	0.044	0.032	-0.6	0.74
0.8	24.	39.	1.2	54.	0.048	0.031	-0.6	0.50
0.8	24.	39.	1.0	40.	0.035	0.025	-0.3	1.00
0.8	24.	39.	0.9	27.	0.029	0.022	-0.6	0.75
0.8	24.	39.	0.9	31.	0.029	0.022	-0.4	0.50